Geomagnetism Applications

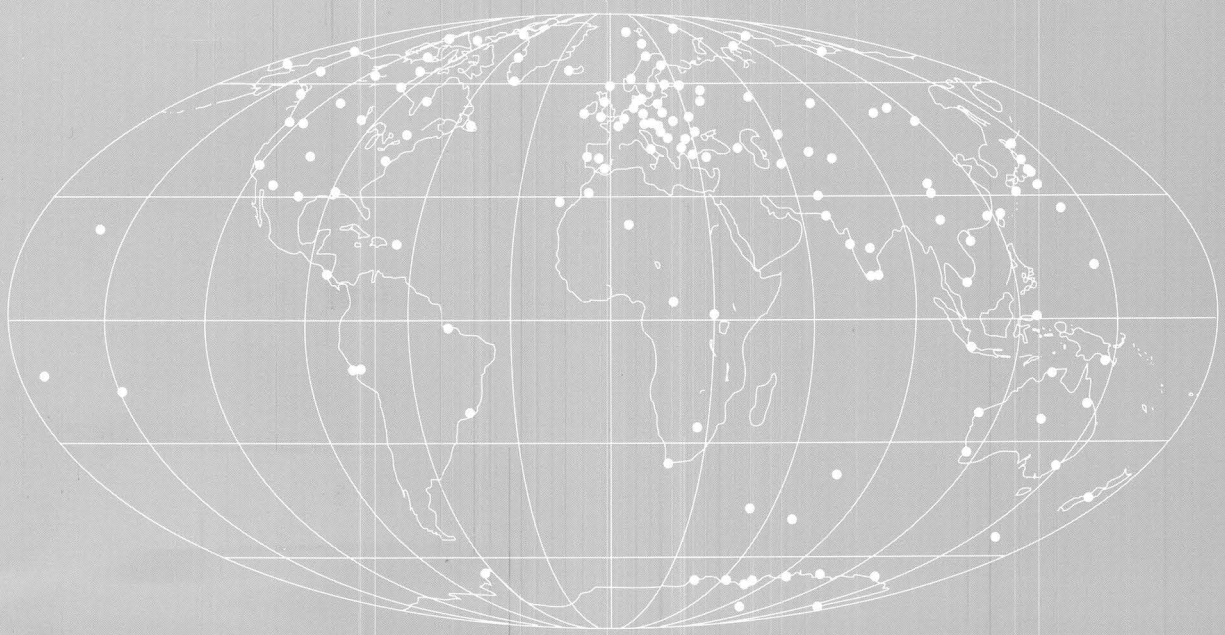

U.S. GEOLOGICAL SURVEY CIRCULAR 1109

Cover. Global magnetic observatory locations depositing records in World Data Center–A in 1994.

Geomagnetism Applications

By Wallace H. Campbell

U.S. GEOLOGICAL SURVEY CIRCULAR 1109

UNITED STATES GOVERNMENT PRINTING OFFICE, WASHINGTON : 1995

U.S. DEPARTMENT OF THE INTERIOR
BRUCE BABBITT, Secretary

U.S. GEOLOGICAL SURVEY
Gordon P. Eaton, Director

Free on application to U.S. Geological Survey, Information Services
Box 25286, Federal Center
Denver, CO 80225

Library of Congress Cataloging-in-Publication Data

Campbell, Wallace H. (Wallace Hall), 1926–
Geomagnetism applications / by Wallace H. Campbell.
p. cm. — (U.S. Geological Survey circular ; 1109)
Includes bibliographical references (p.)
1. Geomagnetism—Industrial applications. I. Title. II. Series.
QC815.2.C36 1995
538′.7—dc20 94-35641
CIP

CONTENTS

FIGURES

TABLES

GEOMAGNETISM APPLICATIONS

By Wallace H. Campbell[1]

ABSTRACT

The societal uses of knowledge acquired from geomagnetism studies include research on space environment and satellite damage, pipeline management, electric power grid failure, communication interference, global position determination, mineral resource detection, Earth formation and structure, navigation, weather, and magnetoreception in organisms. Continuing observation of the geomagnetic field, together with careful archiving of these records and development of mechanisms for disseminating these data, guarantees the enduring utility of geomagnetism studies in today's world.

INTRODUCTION

The observation of the Earth's magnetic field is a modern multiuse technology. Results obtained from such studies are used in many ways. Each period range of natural geomagnetic field fluctuations is applicable to specific areas of study. For example, consider these:

1. From 0.25 seconds to 1 minute: Earth crust exploration, detection of hidden conductivity anomalies, electric power transformer failures, hydromagnetic wave propagation, and revelation of magnetospheric processes.

2. From 1 minute to 24 hours: structure of magnetospheric deformation and currents, thermospheric heating and winds, ionospheric currents and tides, and conductivity characteristics of the Earth mantle and continental coastlines. Geomagnetic storms in this time scale affect a multitude of manmade systems such as satellites, communication systems, electric power grids, and long pipelines.

3. From 1 day to 1 year: fluid motions within the Earth's core and at the core-mantle boundary, solar activity and solar sector changes, tropospheric weather changes, and magnetospheric deformation. Our main-field magnetic navigation charts are obtained from data in this period range.

4. From 1 year to 100 years: changes in the Earth's outer core dynamo-field moment, solar-cycle variability, and climatic variation in solar-weather relationships.

5. From 100 years to 3,000 years: evidence of the Earth's polar wandering, non-dipole outer-core drift patterns, and historic climatic changes from archaeomagnetic and lava-flow magnetic samples.

6. From 3,000 years to 150 million years: main-field reversals and dipole field disappearances, paleomagnetospheres, and continental drift.

The topic of geomagnetism applications is so broad that it is difficult to organize a description. I introduce the subject with a discussion of the uses of geomagnetism in understanding our space environment so that the reader can appreciate the geomagnetic field structure and sources of the major disruptions. Next, I discuss the spectacular effects of geomagnetic storms on satellites, pipelines, electric power grids, communication systems, and geographic position determination. Perhaps not as sensational, but of immediate application, are studies utilizing geomagnetism for surveying the Earth's composition, both for mineral discovery in the crust and for revelation of the Earth's structure. Magnetic charts and navigation represent the more ordinary uses of geomagnetism that do not create headlines in national magazines but form the preponderance of applications to human activity. Interesting possible future directions for geomagnetism applications are the study of global weather and living organisms. I conclude this discussion of geomagnetism applications by providing with some information about observation of the geomagnetic fields and predictions of disturbance.

PHYSICS OF THE EARTH'S SPACE ENVIRONMENT

The Earth has a dipolelike magnetic field called the "main field" that originates from electric currents within the Earth's liquid outer core. These currents probably are driven by a gravitational growth of the inner core and are organized

[1]U.S. Geological Survey, MS 968, Box 25046, Denver, Colorado 80225.

by the spin of the Earth. The dipolelike field defines geomagnetic coordinates at the Earth's surface whose poles are tilted by about 11° with respect to the geographic coordinate system. We have learned all this from the years of carefully maintained records of our Earth's main field and its changes.

The geomagnetic field of the Earth extends its control over charged particle motions far into space, a region that has been named the "magnetosphere." Despite its name, this magnetosphere is not spherical in shape. Although clearly dipolar in form out to several Earth radii (R_e), it assumes a more elongated teardrop appearance near its outer boundary. The outer shape of the magnetosphere is fashioned by a constant arrival of plasma of ionized particles and associated magnetic fields from the Sun called the "solar wind." The first information on this space behavior came from geomagnetic observatory records interpreted early in this century before the advent of satellites.

The Sun is the source of geomagnetic field disturbances. When the phrase "solar-terrestrial activity" is used, the intent is to restrict the subject to those increases of energetic particles and electromagnetic fields that originate at the Sun, travel to the Earth's magnetosphere, and have drastic effects on the Earth's upper atmosphere and geomagnetic field. The activity is on time scales that are short in the human perception of events. The Sun is said to be "active" when the magnitude of such changes is distinguishably large with respect to the average behavior over tens of years.

Uniquely active regions of the solar surface are responsible for the coronal mass ejections of energetic particles and fields. Although relatively random in occurrence, these events that encounter the magnetosphere are organized by a solar activity cycle of about 11 years and by the solar-surface rotation, which has about a 27-day period). Upon intercepting the Earth's magnetosphere, the solar blast of particles and fields blows the Earth's dipole field into an elongated cometlike structure, compressing the day-side geomagnetic field to an 11-R_e position and even past 6 R_e during great storms. The downwind magnetospheric tail extends far past the Moon's 60-R_e orbit. Surface magnetic observatories respond to this distortion of the magnetosphere.

An interplanetary magnetic field travels in the solar wind, defined at the Sun and frozen-in with the solar-ejected particles. When this field that arrives at the day-side magnetosphere is southward in direction, a major geomagnetic storm ensues in which currents of charged particles follow complicated routes through the magnetosphere (fig. 1). This storm is a period of Earth surface field disturbance, recorded at geomagnetic observatories throughout the world.

Individual interrelated magnetospheric and ionospheric processes that occur during the period of a geomagnetic storm are called "substorms" (Rostocker, 1993). Studies of substorms connect the severe changes in the magnetospheric tail region, partial ring currents encircling the Earth, and strong currents that precipitate particles along Earth field lines into the high-latitude auroral region. Auroras occur as this precipitation excites oxygen and nitrogen of the upper atmosphere to glow at the prescribed wavelengths that are allowed by their atomic and molecular structure. In these aurorally active regions the upper atmosphere is heated and the ionospheric conductivity is so enhanced that intense "electrojet" currents flow.

Magnetic observatories throughout the world provide continuous detailed monitoring of the individual processes that transpire in the space about the Earth, a region of major national economic interest. Magnetic data from selected observatories are presently grouped to form global indices of the activity. Auroral electrojet (*AE*) indices are used to describe the critical particle precipitation regions at high latitudes. *Kp* (and *ap* and *Ap* derived from *Kp*) indices follow the general global activity levels. *Dst* indices, from selected middle- and low-latitude stations, represent the averaged distant magnetospheric changes that define a geomagnetic storm (fig. 2). Let us next consider some of the ways that geomagnetic disturbance indicators are useful in quantifying the impact of geomagnetic storms on our present society.

SATELLITE DAMAGE

Onboard computers in space systems orbiting the Earth have lifetimes that are mostly determined by the accumulated radiation damage to their circuitry from energetic particles in the magnetosphere. Solar-cell arrays powering the satellites also lose a few percent of their efficiency each year of solar-terrestrial environment exposure. Storm-time high-latitude field-aligned currents heat the thermosphere causing it to expand upward and move toward the Equator. These thermospheric winds and density increases modify the drag on satellites at their typical equatorial and polar orbiting altitudes near 500 km. The attending decrease in orbital velocity can cause transitory tracking loss and eventually shortens the satellite lifetime.

Synchronous-orbit satellites at about 6.6 R_e commonly experience malfunctions from storm-time solar particle events. During some storms the magnetospheric compression by the solar wind forces the magnetospheric boundary inward past the geostationary satellite position; such transitions have been found to correlate with numerous satellite operation anomalies (Allen and others, 1989). The offset of the geomagnetic and geographic poles and equators (determined from our accurate global magnetic field charting) affects the geographic longitude distribution of particles that produce satellite damage; geostationary longitude placement of spacecraft becomes a compromise location based in part on geomagnetic considerations determined from global field modelling by the U.S. Geological Survey (USGS) and other national organizations.

Allen and Wilkinson (1992) summarized the space effects of the storms of October 19–21, 1989:

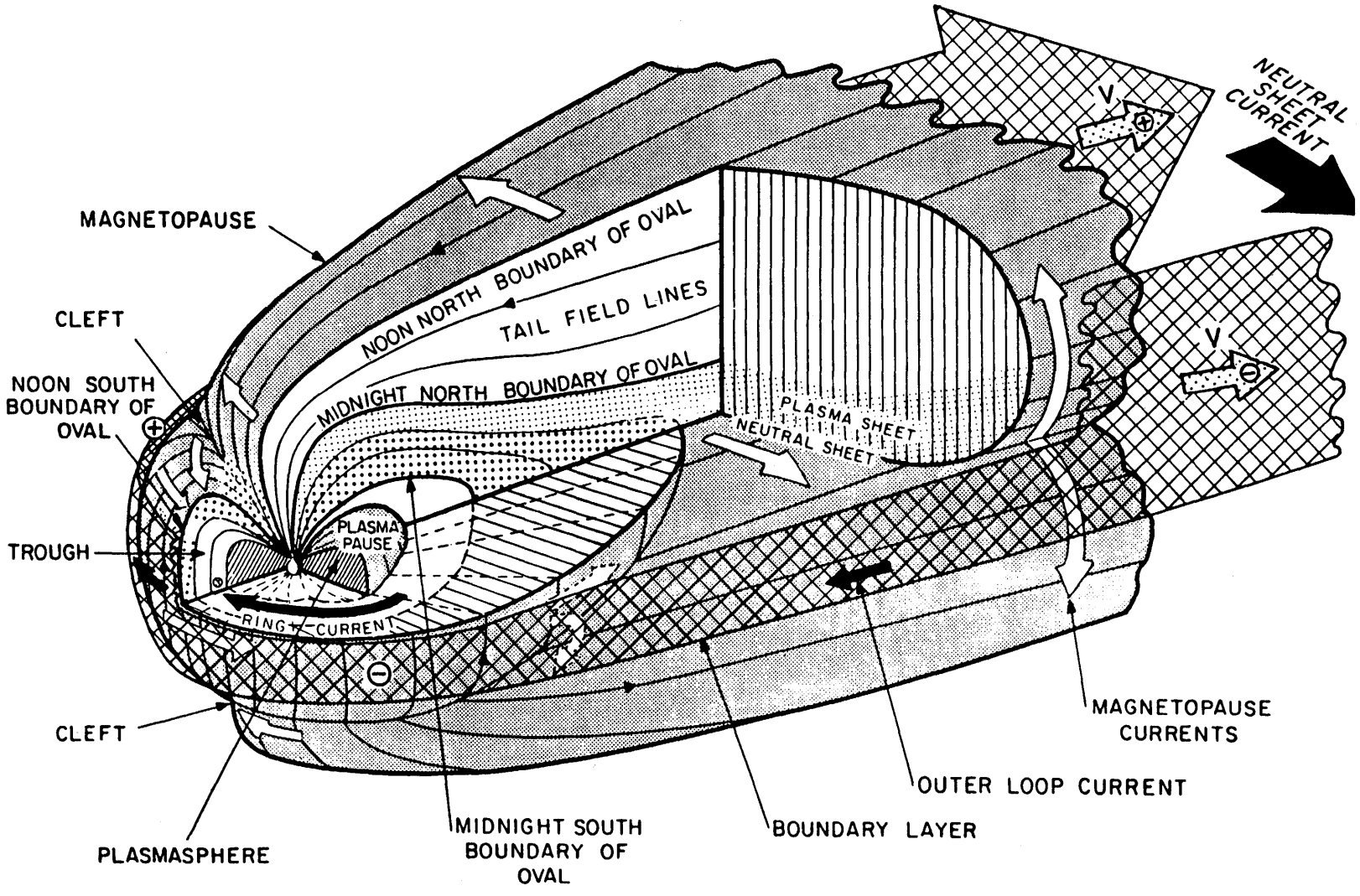

Figure 1. Present model of magnetospheric field distorted by the arrival of disturbed solar wind. Courtesy of World Data Center–A.

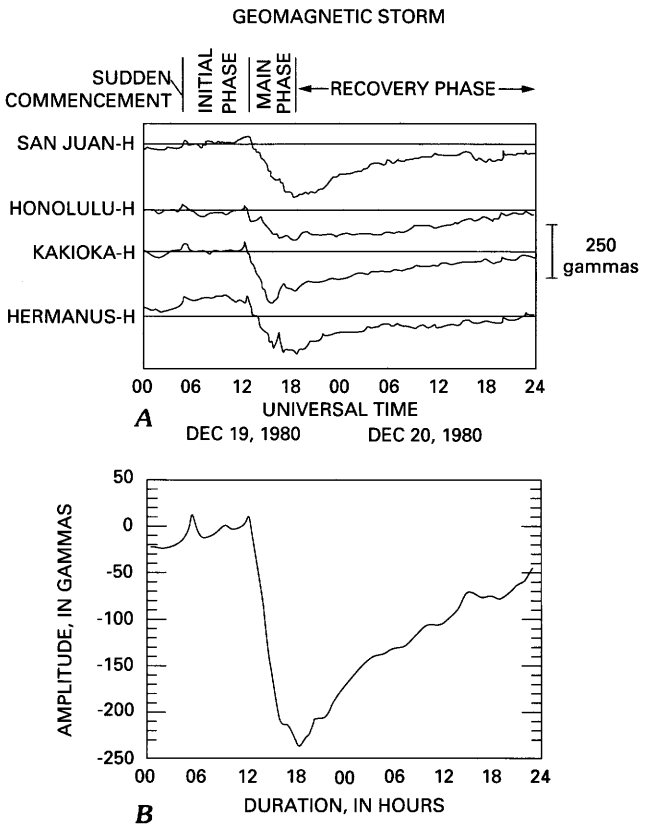

Figure 2. H-component field variations for a geomagnetic storm of December 19, 1980, for the period December 19–20, 1980. *A*, Variation at *Dst* observatories. *B*, Computed *Dst* hourly index.

During the particle events and magnetic storms of this period in October both GOES–5 and –6 experienced SEUs [single particle upsets], polar orbiters experienced multiple switching off of microwave transmitter units—operators quit 'counting' anomalies and just left the system turned off until conditions improved. TDRS–1 had 50 RAM [random access memory] hits on the 19/20th in the radiation susceptible memory chips. Even the hardened TDRS–2 and –3 experienced SEUs. Polar orbiting UOSAT–2 had many SEUs, particularly in the expanded South Atlantic Anomaly region. Significant power panel degradation occurred on GOES–5, –6, and –7. Commercial geostationary satellites had power panel degradation, pitch glitches, and SEUs (137 events reported). Bright red aurora were seen at unusually low latitude over Japan during these events. On October 20–21, Ap* = 162 [Ap* is the maximum 24-hr running mean of the ap index]. . . on board ATLANTIS [space shuttle] the astronauts reported irritating 'flashes' in their eyes as energetic protons penetrated the optic nerves. Although they are reported to have 'retreated' to the innermost shielded part of the Shuttle, the eye flashes did not subside until the proton event ended.

Satellites have been completely disabled during periods of high solar-terrestrial disturbance activity. As an example of major storm-time problems for geostationary satellites, Wrenn (1994) of the U.K. Defense Research Agency reported, "On January 20, 1994, the ANIK E1 and E2 communications spacecraft suffered serious failures of their momentum wheel control systems. It is likely that the satellites were subjected to reduced lifetimes and to bulk revenue losses running into tens of millions of dollars."

Presently, it is thought that failure of spacecraft circuitry is caused by disturbance-time internal dielectric charging of satellite components and the resulting subsequent discharge. Satellite shielding (a major weight-cost consideration) is limited by projected lifetime considerations that rely on the accurate interpretation of past solar-terrestrial disturbance behavior extrapolated from geomagnetic storm information provided by our observatories.

Adequate storm warning systems allow the implementation of protective procedures or a delay of command transmission to more favorable times for some spacecraft. Space shuttle programs have plans to abort extravehicular activities or even the flight itself during major storms to protect astronauts from expected exposures by storm-time particles. The supersonic airplane, *Concorde*, has arrangements to be brought to lower altitudes in extreme, storm-time, exposure-threatening conditions. Real-time geomagnetic field information from selected observatories is an important part of the alarm system used at space-environment forecasting centers.

INDUCTION IN LONG PIPELINES

The Alaska oil pipeline is essentially a 769-mile (1.28×10^3 km)-long, surface-grounded conductor extending from about 69° geomagnetic latitude at the Arctic Ocean to about 62° geomagnetic latitude at the North Pacific Ocean. Those geomagnetic latitudes overlap the auroral zone of intense field-aligned and ionospheric-electrojet currents. The resistance per unit length of the pipe is about 4.8×10^{-6} ohms per meter. Approximately half of the pipe length is buried. The central third of the pipeline parallels the geomagnetic latitude directions favored by the auroral electrojet current. Because of the high pipe conductivity with respect to the ground (to which it is electrically connected by zinc grounding cables), the strong fluctuating ionospheric currents (in the preferred geomagnetic east-west direction) at geomagnetic storm times induce currents to flow in the pipeline. When the pipeline was originally placed in the ground, small cuts in the electrically insulating surface coating occurred. An induced fluctuating current travels between the pipe and ground; when directed appropriately, that current causes pipe corrosion. The amount of corrosion is dependent on the frequency and amplitude of the storm-time source current, the exposed area of the pipe, the material in which the pipe is embedded, the frequency dependence of the corrosion process, and the frequency dependence of the local Earth induction (Campbell, 1986).

For high-latitude pipelines such as those in Alaska and Canada, the effect of corrosion from the induced geomagnetic storm current maximizes with the 5–30-minute period field fluctuations. Figure 3 shows the correspondence of pipe to soil currents and geomagnetic activity for a high-latitude pipeline. During large storms induced currents in the

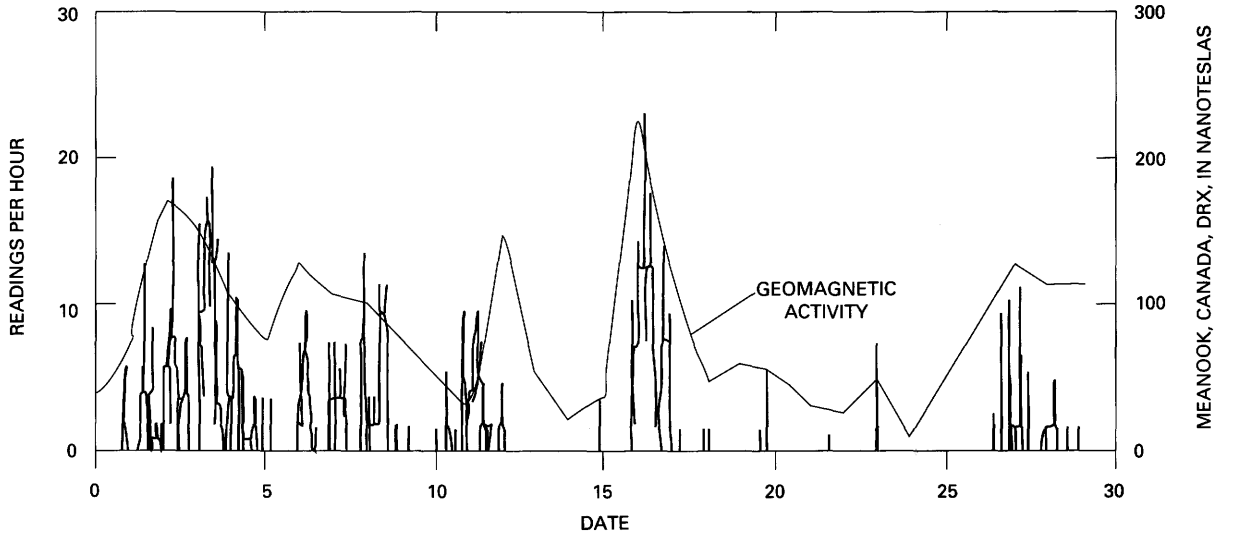

Figure 3. Comparison of pipe-to-soil current (vertical line segments) on the Leismer Gas pipeline system northeast of Edmonton, Canada, and geomagnetic field changes. DRX is the daily range of the *X* component. Modified from Shapka (1993).

pipelines can be as high as as 1,000 amperes. Estimates of corrosion effects over the lifetime of the Alaska pipe were obtained by comparison of presently measured pipeline currents with the USGS College and Barrow observatory magnetic field records and an extrapolation of the field's historic behavior. It is believed that the high-latitude pipelines are corroding faster than originally anticipated because induced currents were not adequately taken into consideration in the original design. Only recently did some pipeline companies begin measuring these induced currents to institute corrective procedures.

At all latitudes, pipeline corrosion is also caused by the steady currents generated either from the difference in contact potential at grounded points in the pipeline or from the induction of currents from nearby manmade systems. Most pipelines are protected from this harmful current by application of an overriding current sent onto the pipe to make all exposed areas negative (a cathode) with respect to ground. Corrosion engineers have regularly scheduled surveys of their pipeline potential to adjust their cathodic protection devices. Geomagnetic storms give rise to induced currents in all pipelines throughout the world. If the corrosion engineer surveys are made during geomagnetic storms, improper cathodic protection voltage levels may actually cause an increase in corrosion.

Near dip equator locations, strong daytime electrojet ionospheric current fields and enhancement of low-latitude geomagnetic storm fields induce strong currents to flow in the pipelines that parallel the electrojet. The great intensity of these equatorial source currents exacerbates corrosion compared to higher latitudes, and greater attention must be paid to cathodic protection devices. The equatorial regions of intense induced currents are determined by geomagnetic surveys.

Geomagnetic data from USGS observatories help make it possible for the National Oceanic and Atmospheric Administration (NOAA) Space Environment Forecast Center to warn U.S. pipeline management companies of the present and expected activity levels that are of importance to their corrosion protection methods.

INDUCTION IN ELECTRIC POWER GRIDS

During severe magnetic storms ($Kp \geq 7$), damaging currents can be induced in power grids, particularly at higher latitudes. The effects vary from simple tripping of circuit breakers resulting in temporary electric power blackouts of cities to destruction of expensive power station transformer banks and major economic loss from extensive private and industrial power disruption. The problem occurs when storm-induced currents appear in three-phase transformers that are electrically connected by long transmission lines. Destructive localized heating occurs in the windings, capacitor banks become overloaded and trip out, protective relays fail, and power transmission is degraded or lost completely.

As an example, on August 4, 1972, a large geomagnetic storm ($Kp=9_0$) caused the failure of a 230-kV power transformer at the British Columbia Hydro and Power Authority of Canada. During the great magnetic storm ($Kp=9+$) on March 13, 1989, major field fluctuations centered near southeastern Canada and the northeastern United States caused a 9-hour blackout of the 21,000-MW Hydro Quebec electric power system. A vivid description of the failure was provided by Blais and Metsa (1993) of Hydro-Quebec.

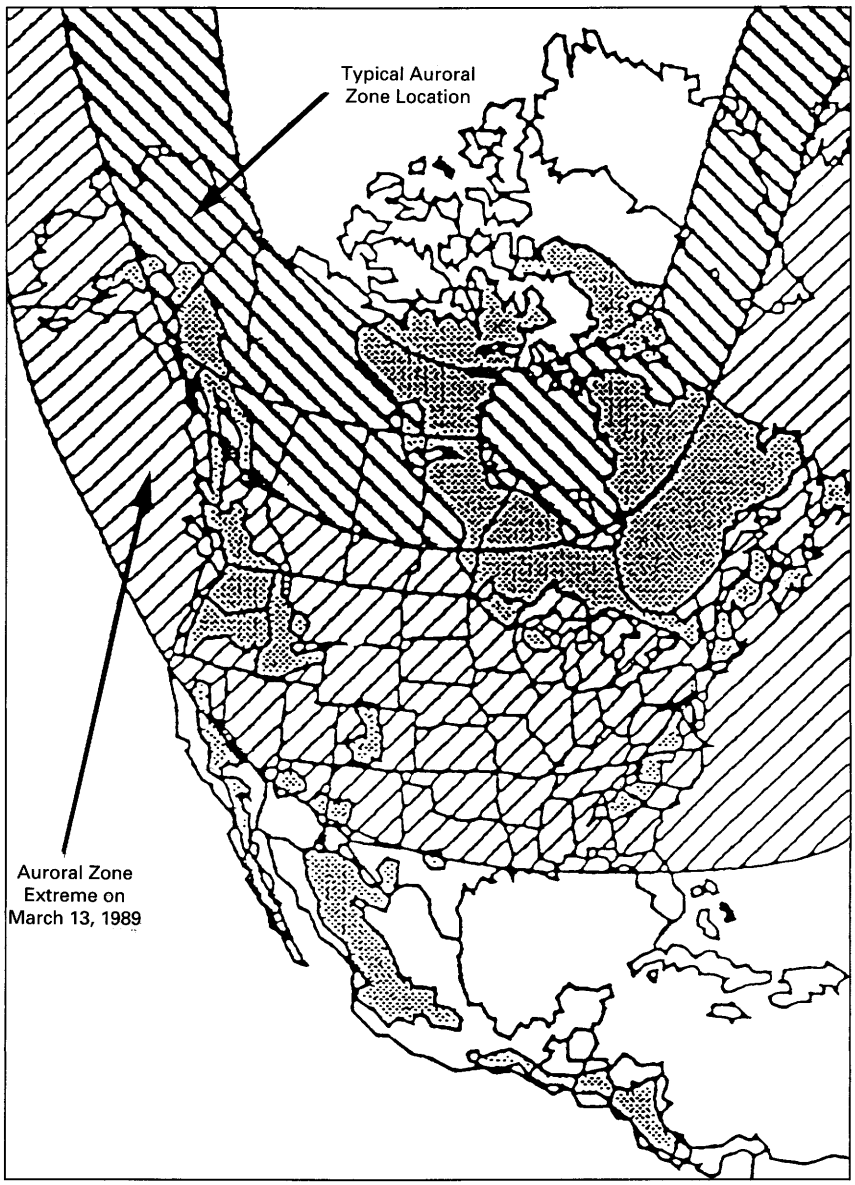

Figure 4. Areas of igneous rocks (shaded area) and auroral zone (diagonal-lined area). Interconnected power systems are vulnerable in the overlapping regions during geomagnetic storms. Modified from Kappenman (1992).

Telluric currents induced by the storm created harmonic voltages and currents of considerable intensity on the La Grande network. Voltage asymmetry on the 735-kV network reached 15 percent. Within less than a minute, the seven La Grande network static var compensators on line tripped one after the other . . . With the loss of the last static var compensator, voltage dropped so drastically on the La Grande network (0.2 p.u.) that all five lines to Montreal tripped through loss of synchronism (virtual fault), and the entire network separated. The loss of 9,450 MW of generation provoked a very rapid drop in frequency at load-centre substations. Automatic underfrequency load-shedding controls functioned properly, but they are not designed for recovery from a generation loss equivalent to about half system load. The rest of the grid collapsed piece by piece in 25 seconds.

Power pools serving the entire northeastern United States also came perilously close to a comparable calamity with similar cascading system failures during the same geomagnetic storm that affected Hydro-Quebec. In addition, the storm destroyed transformers at the Salem Nuclear Plant of the Public Service Electric and Gas Company, at a replacement cost of about $12,000,000. During this loss of power output, the PSEGC replacement energy cost was approximately $400,000.

Power-grid vulnerability is dependent on the nearness to a region of maximum auroral electrojet currents, the interconnection pattern of the power-grid system, and the regional geology of high-resistance igneous rock. Figure 4 illustrates the regions of concern for North America. The rapidly fluctuating storm-time induced currents are thought to enter and exit power systems through the grounded

connection of transformers, causing a high level of half-cycle saturation and dramatically increasing reactive power consumption and localized destructive heating; intolerable system voltage depression, unusual transmission line flow, and relay malfunction follow.

Present protection strategies for power companies to deal with geomagnetically induced currents (GIC's) involve both system redesign, based on the history of geomagnetic field at the critical locations over a solar cycle, and adequate warning of impending storm onsets and recovery times. Improvements in geomagnetic storm forecasting mostly depend on expansion of the global geomagnetic information real-time network (INTERMAGNET, described in the section on "Magnetic Observatories"), as well as careful reanalysis of past records.

COMMUNICATION SYSTEMS

Modern communication systems rely primarily on satellite transponders, radiowave links, oceanic and land-based cables, telephone line connections, microwave transponders, and fiber-optic cables. Even though the last two apparently are not susceptible to geomagnetic storm induction problems, the universal interconnection of transmission facilities brings problems to all systems. First realization of major communication problems began with unmanageable induced voltages on telegraph lines during a severe geomagnetic storm period of August 28 to September 4, 1859. As an example of troubles in more recent years, 80 percent of all long-distant telephones in Minneapolis were silenced by the great (Kp=9$_0$) magnetic storm of March 24, 1940. At the same time Bell System's transatlantic cable experience significant difficulties when an estimated 2,650 volts appeared across the line. The major (Kp=9$_0$) geomagnetic storm of February 10, 1958, induced 2,700 volts on the Bell System cable from Newfoundland to Scotland and fluctuated voice communications from "squawks to whispers" (Lanzerotti and Medford, 1989). The magnetic storm of August 4, 1972 shut down a "Long-Haul" coaxial communications cable between the States of Illinois and Iowa. Storm-time induced current fluctuations on communication cables that do not fail nevertheless cause problems in business digital data and facsimile transmissions.

At high latitudes, satellite transionospheric radiowave signals during storms suffer from refraction and rotation of the signal plane of polarization related to severe changes in total electron content along the propagation path. Storm-time signal phase and amplitude radiowave scintillations disrupt both satellite (at 10^9 Hz) and surface high-frequency (HF) communications. The scintillations arise from scattering by ionization irregularities in the altitudes above 200 km when the ionosphere is dense and unstable during geomagnetic storms.

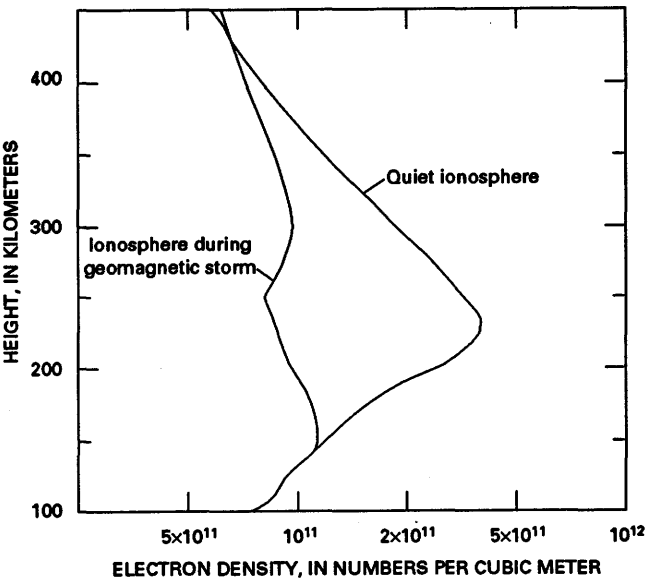

Figure 5. Electron density profiles at middle latitudes during daytime quiet and disturbed geomagnetic conditions. Modified from Norton (1969).

Geomagnetic storm conditions upset the expected pattern of received signals at those radiowave transmission frequencies that depend on the ionosphere as a reflecting medium. This problem is particularly severe at auroral and polar latitudes where the ionospheric conductivity is greatly enhanced during storm conditions. In the past, these regions were not near major population areas, but demographic changes have increased national dependence on high-latitude communications. At lower latitudes the storms are responsible for phase changes in the very low frequency (VLF) navigation systems, fadeouts of short-wave communication links, and major modification of usable radio frequencies. Global ionospheric models used for prediction of the propagation conditions all need geomagnetic disturbance indices for critical adjustments.

Both the F-region and total electron content (TEC) of the ionosphere are adversely affected during geomagnetic storms, but the relationship are not easily predicted. At times there is an increase in ionization in the morning hours and a severe decrease in the evening (fig. 5). Small storms can sometimes cause major disruption of the total electron content. Figure 6 illustrates the degradation of high-frequency (HF) radio propagation quality for fixed-frequency station transmissions along six representative transmission paths during a severe magnetic storm period in March 1990.

Some transmitters have flexibility in the selection of the broadcast frequencies. For these, the usable frequency is predicted from Ap index values computed from the geomagnetic records and disseminated by the forecasting centers. In addition to government and industrial broadcasters, more than 1 million amateur radio operators in the world make use of geomagnetic storm "nowcasts" and forecasts.

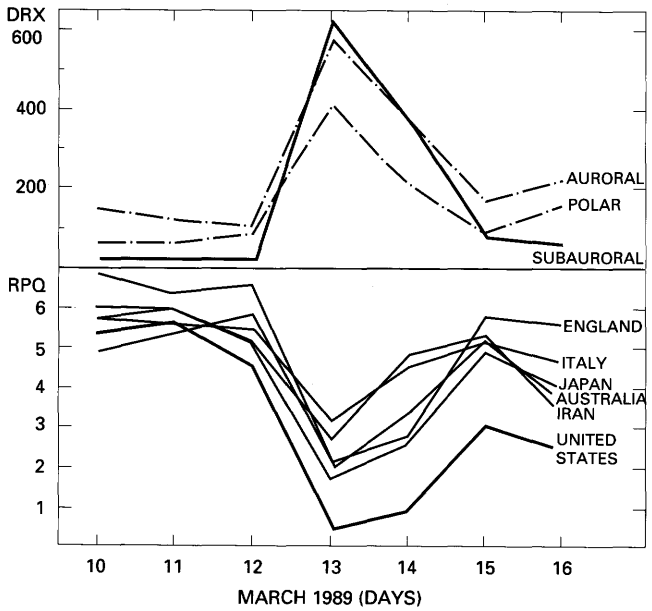

Figure 6. Correspondence of the daily range of the *X*-field component (DRX, in nanoteslas) in subauroral, auroral, and polar cap zones to the radiowave propagation quality index (RPQ) for paths from western Germany to the United States, Iran, Australia, Japan, Italy, and England during a geomagnetic storm period in March 1989. Modified from Hruska and others (1990).

GLOBAL POSITIONING SYSTEM

The Global Positioning System (GPS) now used for navigation and surveying depends on propagation-time delays for spread-spectrum signals transmitted by 24 satellites. These satellites are in six separate, near-circular orbital planes at an altitude of about 20,000 km. Signals from at least four can be received at any given point near the Earth's surface. The signals, detected simultaneously by the user's uniquely designed GPS receiver, are automatically processed to determine global position. For authorized government users, accuracy is expected to be 8 m absolute position and to be 3 mm relative position between two locations. For unrestricted users of the system (mostly boat and ship navigation), the accuracy is expected to be 50 m absolute and 5 m relative.

During a geomagnetic storm a disturbed ionosphere introduces into the propagation of the encoded signals irregular delays that are proportional to the total ionospheric electron content along the propagation path and inversely proportional to the square of the carrier signal frequency. Propagation delays due to geomagnetic storms can represent errors of 100 m in position (Kleusberg, 1993). Storm notifications from warning centers, employing real-time data from geomagnetic observatories, alert GPS subscribers to positioning error periods during which GPS fixes are unreliable and corrective measures need be considered. Ionospheric modelers compute corrections from the available geomagnetic activity indices. During some geomagnetic storm conditions, rapid variations (scintillations) introduced by the ionosphere also do damage to the position reckoning. Figure 7 shows, for one month in 1987, the occurrence of GPS problems at times of high geomagnetic field levels.

CONDUCTIVITY STRUCTURE OF THE EARTH

Two interrelated geomagnetic methods are used in the study of the Earth's electrical conductivity. In one method, magnetic irregularities caused by various crustal deposits are determined by an area survey. The embedded materials provide the field changes and can be best interpreted when the geomagnetic activity (a noise source) is as low as possible. For proper evaluation of surface surveys for crustal magnetic irregularities, the contribution from the Earth's main field must be removed. Typically, the International Geomagnetic Reference Field or Definitive Geomagnetic Reference Field (IGRF and DGRF, prepared with field models designed by USGS and other national organizations) representation of the main field in the study region is subtracted from the data set.

In the other method, natural geomagnetic field fluctuations due to source and induced currents are interpreted to give a multidimensional crustal conductivity structure or a one-dimentional profile of the upper mantle. A disturbed field is required to provide the frequencies for probing the Earth's crustal layers, and long-wavelength quiet-field variations are used to probe deeper, into the Earth's mantle.

SURFACE AREA TRAVERSES

Magnetic irregularities occur because of the variation in the percentage of magnetite (Fe_3O_4) or related minerals in the Earth. Magnetite is present in most rocks, although perhaps just very small amounts. Both permanent and induced magnetization are the principal sources of fields for these surveys. Surveys are normally performed in geomagnetically quiet times. Compensation for quiet-field variations are obtained by subtraction of the variations determined from a stationary, local baseline field magnetometer (commonly at a standard geomagnetic observatory). The profiling method depends on the changes in magnetic response resulting from the variations in amount of buried magnetite. Occasionally, horizontal gradient measurements are appropriate. Proper interpretation of the surveys depends on accurate collation of the magnetic information with surface geology, gravity records, and seismic profiles.

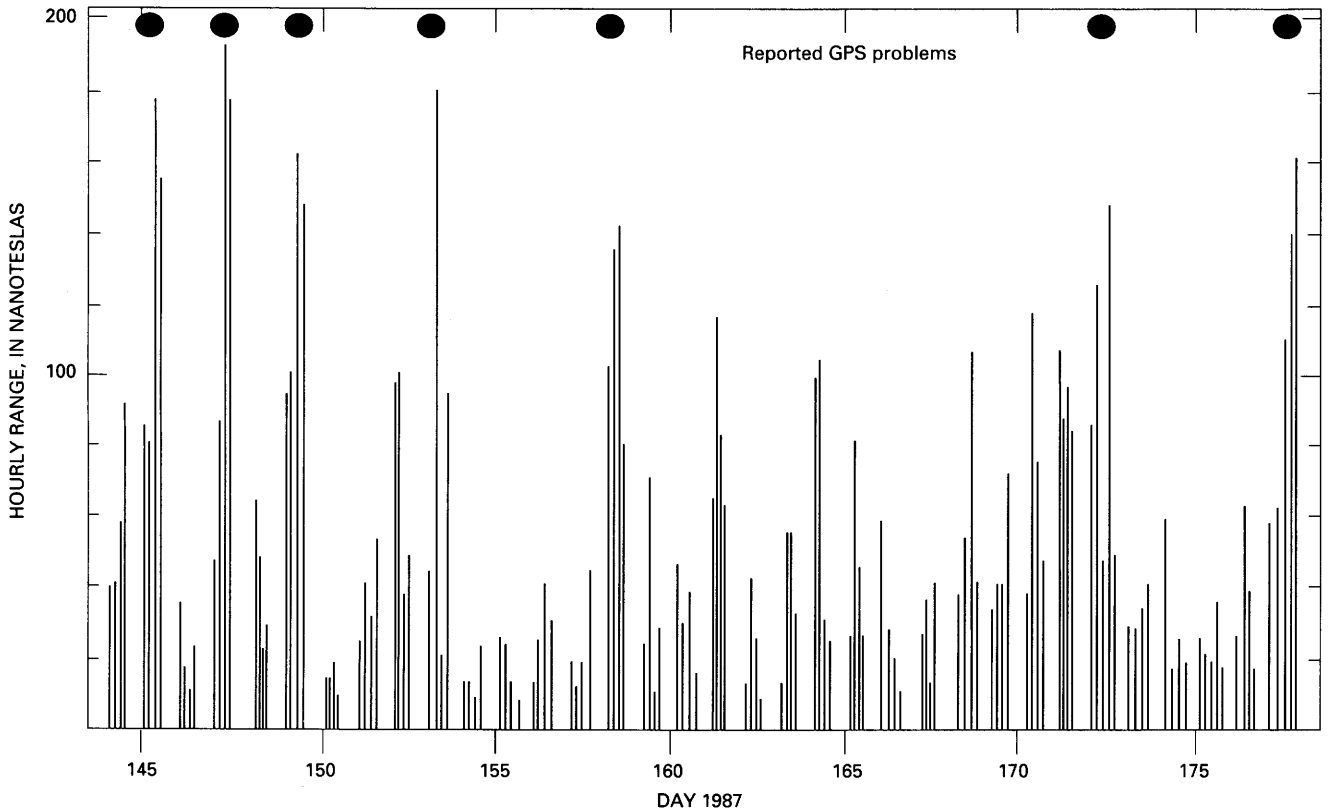

Figure 7. Occurrence of Global Positioning System (GPS) problems (solid circles) and large hourly range of geomagnetic field variation (vertical lines) reported in 1987 by R.L. Coles (Geophysics Division, Geological Survey of Canada, Ottawa).

Some small-area traverses are simply interpreted from the change in field strength and direction as the sensor is moved along a given line. Figure 8 illustrates the different responses of a magnetometer for a simple magnetite alignment. In addition to surveys for mineral discovery and geological interest, buried archaeological formations have been revealed by magnetic surveys of this type. The detection is facilitated by the fact that manmade structures are typically of simple geometric design, consistently of one material differing from that of the immediate general area, and at shallow depth. The contrasting magnetic properties of archaeological interest are, as a rule, easily detected in the uniform overburden of soil, water, or rocks.

A more precise electromagnetic technique for determining the location of anomalous structures in the Earth is called "geomagnetic depth sounding" (GDS). This method uses the three orthogonal magnetic field components and is the favored means for studies using a large-area array of temporary observing sites. Appropriate equations relate the vertical *Z*-component field to the horizontal (*H*) and depth (*D*), or *X* and *Y*, components for each source frequency. Conducting structures are interpreted using special contour plots of the region (Gough and Ingram, 1983).

AEROMAGNETIC SURVEYS

In an aircraft, a magnetometer is subject to contaminating magnetic fields from four sources within the plane (assuming that flight personnel take care with their apparel): (1) permanently magnetized aircraft parts, (2) parts whose magnetization is induced from the presence of the Earth's main field, (3) currents generated in electrically conducting materials (eddy currents) as the plane moves through the Earth's main field, and (4) fields from the changing static charge arising from the plane in flight. Adequate compensation for each of these contaminants is a serious concern of all aeromagnetic programs. Compensation methods involve placement of permaloy strips and current carrying coils near and about the geomagnetic field sensor head and (or) computer program adjustments to the output registration.

To determine the compensation values for aircraft, prescribed airswings are made over a major magnetic observatory. The airborne magnetometer responses are evaluated with respect to the speed, yaw, pitch, and roll of the aircraft in the four cardinal directions. Calibration flights, as well as surveys, are made on geomagnetically quiet days, and to avoid the costly repeat of measurement along flight tracks flight planning depends on reports of concurrent and predicted activity from geomagnetic observatories and forecasting centers.

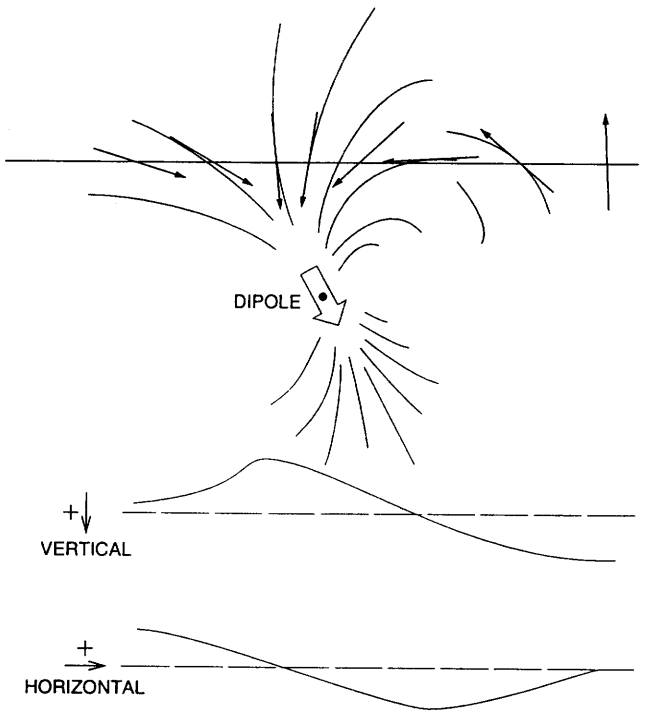

Figure 8. Surface magnetic field response from buried magnetic material exhibiting dipole magnetization.

The first type of magnetic field contamination source, fixed magnetization, requires a permanent adjustment for an unchanged plane configuration, but the effect must be regularly reevaluated because physical shock to the aircraft (such as from a hard landing) can change the magnetization to a new local-field arrangement. Periodic recalibration airswings over the observatory are important. The second type of contamination, induced magnetization, can be evaluated for the calibration flight paths, but the induction effect changes for each survey region in which the Earth's main field is significantly different. The third type of contamination should be evaluated in a manner similar to that for the second with the addition of calibrations for the usual aeromagnetic cruising speeds. The fourth type of contamination, fields from in-flight static charge buildup and dissipation, is difficult to compensate because charge variations follow weather conditions; the range of contamination can be discovered through a comparison of magnetometer readings from overflights of the fixed observatory location in a variety of weather situations.

The most extensive regional aeromagnetic surveys have been made by the U.S. Navy to support production of global magnetic charts of importance for navigation. Figure 9 illustrates the coverage of this global aeromagnetic data set now available from the magnetic field archives at the National Geophysical Data Center (NGDC/NOAA) from its Project Magnet program from 1950 through 1990. These surveys were made at high levels, usually between 15,000 and 25,000 ft (4.6–7.6 km) elevation. Over the years, navigational accuracies have increased from ±5 nautical miles (9.3 km) to ±100 m. Three-component fluxgate magnetometers calibrated with an optically pumped metastable helium magnetometer gave Project Magnet field determination accuracies of approximately ±15 gammas. Project Magnet is continuing with improved system technology providing greater field accuracy.

High-resolution flights for detailed geomagnetic surveys typically are flown at altitudes between about 500 and 1,000 ft (152–305 m). Flight-line separations are estimated to be about twice the distance, *B–A*, from the geological magnetic basement (*B*) to the aircraft (*A*). The sample interval is, by rule, less than one-fourth of *B–A*. Flights are usually restricted to the quieter geomagnetic activity days using disturbance information from the nearest geomagnetic observatories and activity predictions from the space environment forecasting centers.

Three methods are used for adjustment of the flight-time measurements to the variations in geomagnetic activity. (1) Mapped fields are taken to be the difference between the observation and the field measured at a base station magnetometer. (2) With a checkerboard-grid flight pattern, adjustments are applied to bring the crosstrack values into accord; these adjustments define linear alterations of the remaining data samples. (3) Best estimates of the quiet-day field variation (*Sq*) defined for each data sample location and time are removed from the data. *Sq* can be obtained from a local magnetic observatory or, in absence of such a base station, from a program, WDCA–SQ1, developed by the USGS (Campbell and others, 1989) and available from World Data Center–A.

Figure 10 illustrates the aeromagnetic evidence of a major seamount. Figure 11 depicts the magnetic contouring used in determination of the regional geology of the State of Minnesota. Hydrothermal alteration and metamorphism can modify crustal magnetization. Magnetic anomaly maps showing these changes are used in the detection of energy and mineral resources. Aeromagnetically detected anomalies over oil-bearing layers have been interpreted as due to magnetite that formed from chemical processes as a result of microseepage of the petroleum. Oil and gas production fields of the Alaskan Navarin Basin and the European North Sea Basin were discovered using aeromagnetic surveys. Improvements in aeromagnetic techniques over the years have increased mapping contour intervals from a "standard sensitivity" of 10 gammas, to a "medium sensitivity" of near 1 gamma, to a "high sensitivity" of about 0.1 gammas.

SHIP-TOWED MAGNETOMETERS

Unequivocal evidence of continental drift, tectonic motion, and sea-floor spreading was obtained from

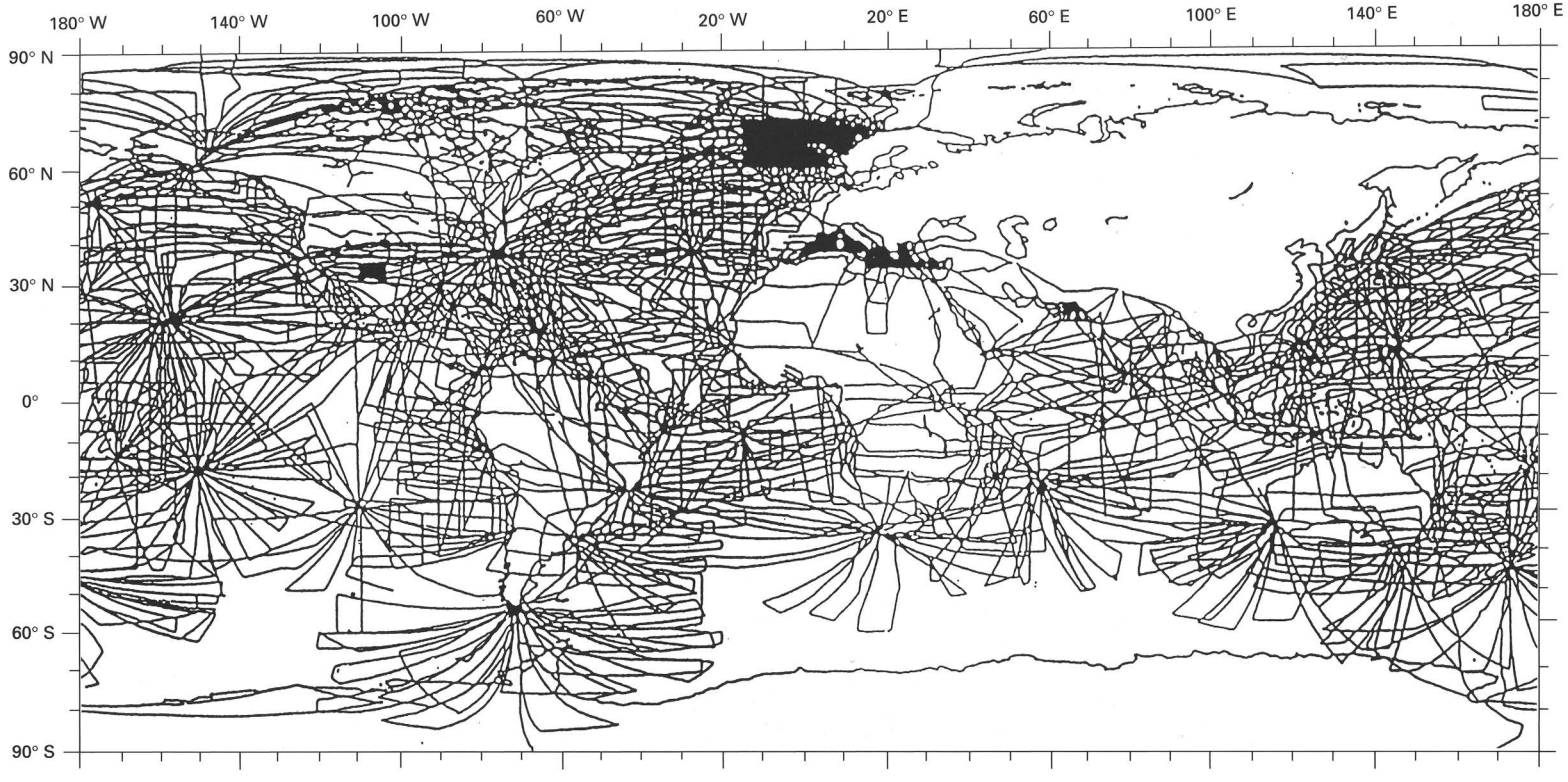

Figure 9. Tracks of U.S. Navy Project Magnet flights for which data were deposited at National Oceanic and Atmospheric Administration National Geophysical Data Center. Courtesy of R. Buhmann (World Data Center–A, 1994).

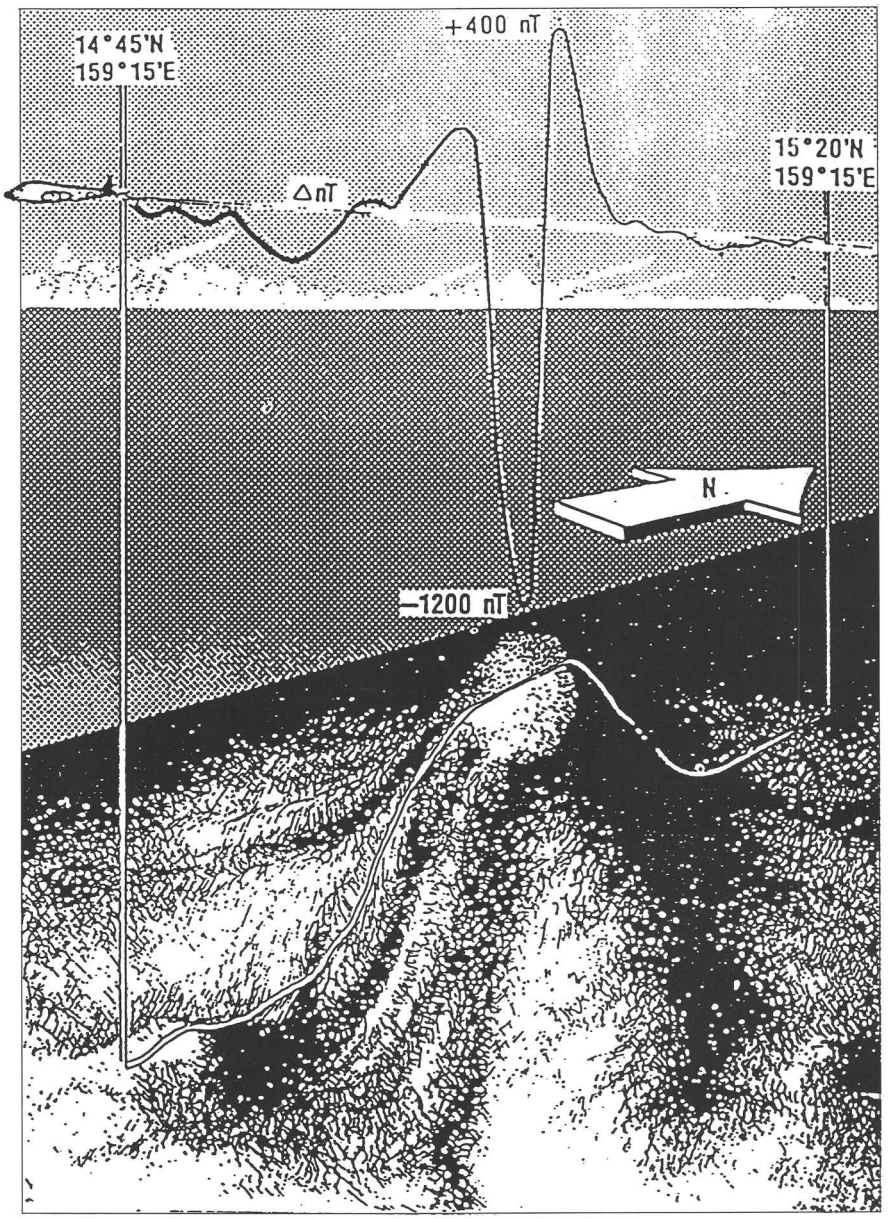

Figure 10. Schematic representation of the detection of seamounts using aeromagnetic techniques. From U.S. Naval Ocean Research and Development Activity report (1993).

ocean-bottom magnetic records. In both directions perpendicular to mid-oceanic ridges, ship-towed magnetometers have detected symmetric patterns of magnetization that were acquired during cooling of hot magma coming from spreading-region mid-oceanic ridges just tens of meters wide. Since the first discovery of the patterns, national geomagnetic programs for ship-towed magnetic surveys (fig. 12) have had as their objective the global establishment of the chronologies for sea-floor geomagnetic polarity changes so that the structure and evolution of the sea floor can be understood.

The magnetometers are usually towed at about 500–1,000 ft (152–305 m) from the vessel. Ocean surface measurements are made at about 50 ft (15 m) below the surface for stabilization. Ocean-bottom magnetometers have been towed at dephts of about 3,000 ft (914 m). On occasion, gradient determinations are made with separated sensors towed in line. Compensation for the permanent and induced magnetization of the ship and for eddy currents is similar to that for aircraft, although greatly different in magnitude, and relies on standard geomagnetic observatory calibration.

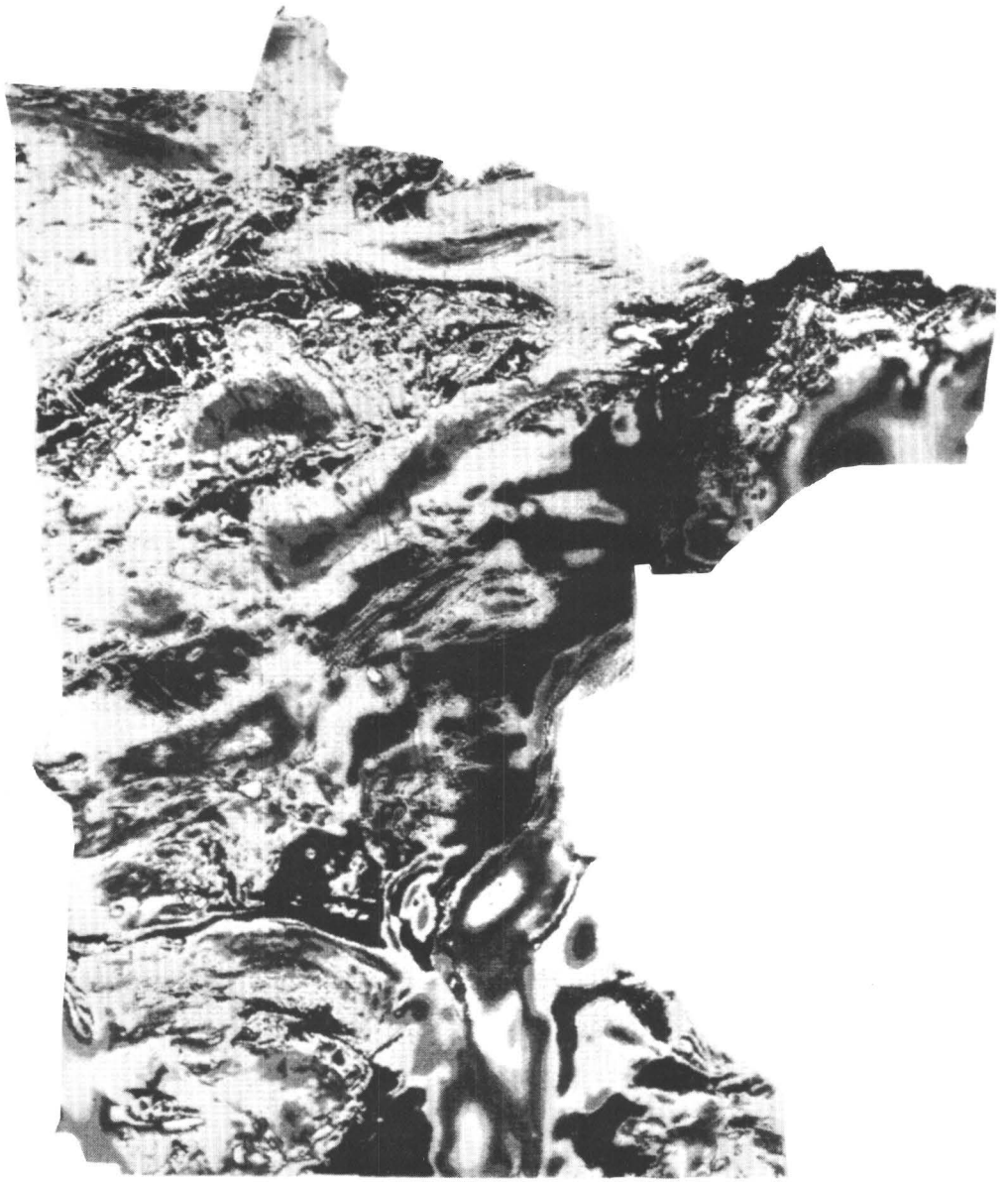

Figure 11. Field contour chart for the State of Minnesota compiled from aeromagnetic data stored at the National Oceanic and Atmospheric Administration National Geophysical Data Center. Courtesy of R. Buhmann (World Data Center–A, 1994).

Both proton (total-field) magnetometers and the combination of fluxgate (vector) and proton (for calibrating the fluxgate) magnetometers are used in ship-towed systems. Ship-towed recordings have been valuable in augmenting the data base for global magnetic field modeling. As knowledge of the geology of continental margins has become increasingly important for oil exploration, shipborne magnetic surveys of the coastal regions have gained further significance.

MAGNETOTELLURIC SOUNDING OF THE EARTH'S CRUST

Remote sensing of the Earth's subsurface crustal structure is an important part of the commercial development of mineral and energy resources. One discovery technique involves determination of the ratio of orthogonal surface electric and magnetic fields to resolve the electric conductivity (siemens per meter) or resistivity (ohm-meters) profile of the Earth beneath the measurements.

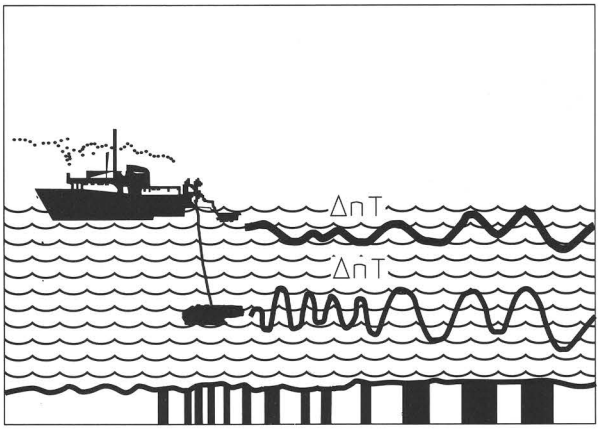

Figure 12. Schematic of ship-towed magnetometers responding to ocean-bottom magnetic striations from sea-floor spreading of magma with frozen-in field alignments. From U.S. Naval Ocean Research and Development Activity report (1993).

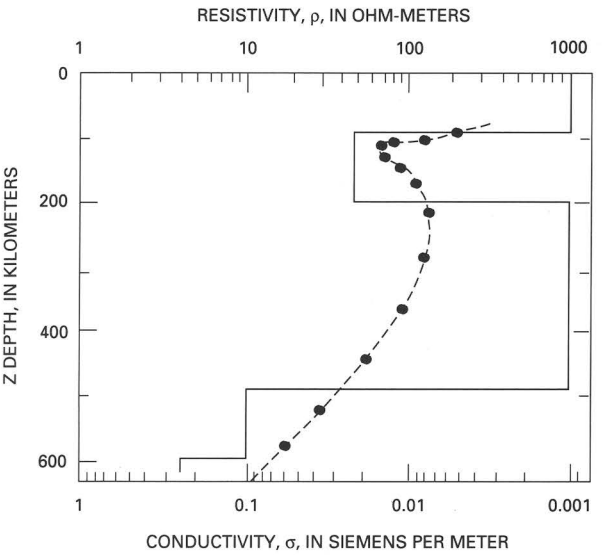

Figure 13. One-dimensional inversion of magnetotelluric data to show conductivity (or resistivity) as function of depth. Dashed line is smoothed form computation (dots). Solid line represents conductivity model structure. Modified from Schmucker (1970).

To provide some understanding of the method, let us consider the following. The currents that are induced to flow in the conducting Earth decrease with the oscillation period and with the depth into the conductor. The parameter, δ, called the "skin depth," defines the distance within a uniformly conducting Earth at which the diminishing field of oscillating period, T seconds, reaches $1/e$ (about 37 percent) of its surface amplitude (where e=2.71828...). The attenuation of source signal with depth into the Earth is similar to the radiowave fading experienced by an auto driver listening to his radio on entering a tunnel. In addition to a period-amplitude relationship, there is a phase rotation of the electromagnetic wave as it penetrates the conducting medium.

Measurements at the Earth's surface give the sum of the induced and source fields. The ratio of the phase and amplitude of the surface electric and magnetic fields provides the specific information on the interior conducting Earth structure. In operation, this method of determining electric conductivity has been named "magnetotelluric" (MT) sounding for the combination of magnetic and telluric fields that are used. The equations that allow us to convert (transfer) the field measurements into conductivity are called "transfer functions."

To a first rough approximation in the region of the measurement, the apparent conductivity, σ, in siemens per meter, is

$$\sigma \approx \frac{5}{T}\left|\frac{B_y}{E_x}\right|^2$$

where T is the field fluctuation period in seconds, B_y is the magnetic field in gammas, and E_x is the electric field in millivolts per kilometer (the subscripts x and y refer to orthogonal directions). In a given conductivity half-space, longer period field fluctuations penetrate to greater depths. The apparent conductivity thus determined is assumed to be valid to a penetration depth of Z kilometers approximately given by

$$Z \approx \frac{1}{2\pi}\sqrt{\frac{5T}{\sigma}}.$$

Present analysis techniques are considerably more complex than these equations indicate. The relationship of both the amplitude and phase of the electric and magnetic fields enters the more exact computations. With observations at a multitude of frequencies, a depth profile of the apparent conductivity for the region is obtained. This profile is taken to be a smoothed representation of the true conductivity. A model structure of the crust is then adopted with an appropriate depth scale to fit the MT profile (fig. 13). Processing the data in this way is called "MT inversion" (Oldenburg, 1990).

The interrelationship of the magnetic and electric (telluric) field (MT) vectors is substantially more intricate for the realistic anisotropic and laterally inhomogeneous Earth in which conductivity must be represented as a function of directions other than depth. The problem resolves into modeling minimum-structure arrangements of conducting masses of defined boundaries in two or three dimensions (called 2D or 3D models). Figure 14 illustrates the 2D model of the Juan de Fuca plate subduction zone of southwestern Canada obtained from a combination of MT and GDS survey techniques.

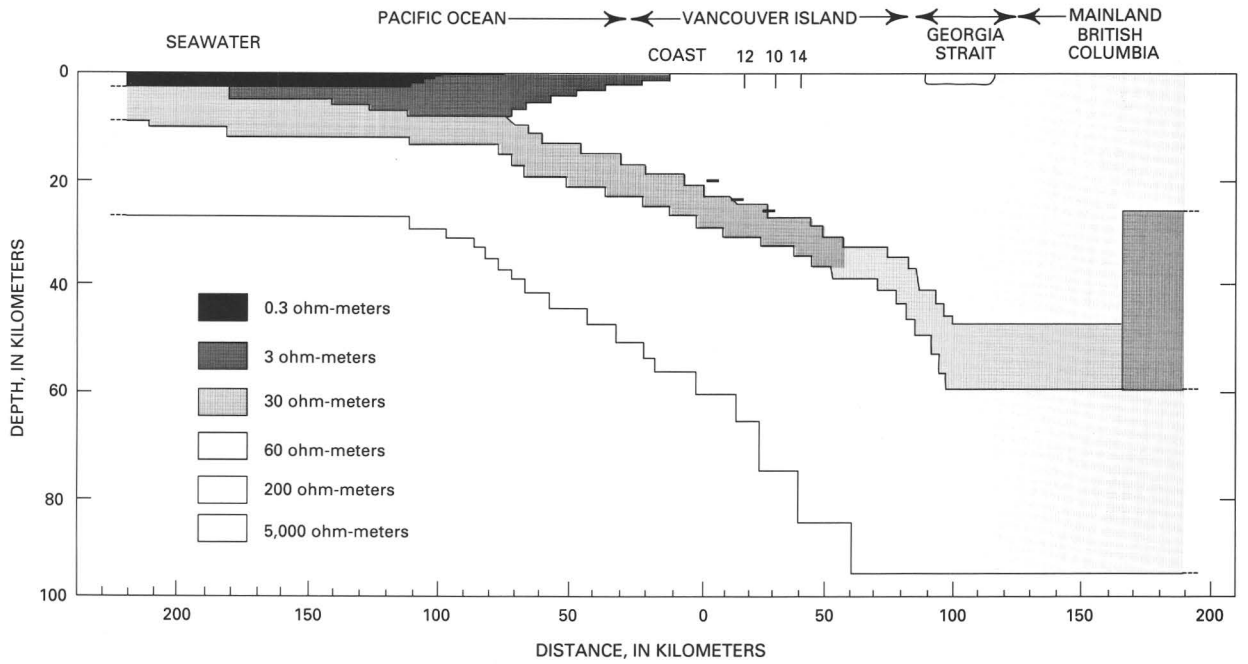

Figure 14. 2D electrical resistivity model of Juan de Fuca plate subduction region near Vancouver Island, Canada. Black horizontal bars beneath sites 10, 12, and 14 on Vancouver Island indicate the seismic reflector location. Modified from Kurtz and others (1990).

There are always measurement errors, so the data cannot be fit exactly. Often more than one model will satisfy the MT responses. Special techniques have been developed to evaluate the misfit between the data and the model. Usually, the true distribution of conducting materials is not obtainable, nor is the true error of the computations. Therefore, there is always considerable reliance on a comparison with seismic evidence of the Earth's substructure; major changes at specific depths must be collocated. Inverse modeling accuracy also depends on the detailed laboratory measurement of geologic material conductivities.

Natural micropulsation field variations, which have a wide range of frequencies and great horizontal uniformity (at least at latitudes away from the auroral zones), are a convenient source field in the application of magnetotelluric prospecting techniques. Although crustal modeling concerns the first 10 km below the Earth's surface, reliable conductivity determinations have been extended to about 200 km. The MT method is used principally for mineral discovery, geothermal prospecting, and general evaluation of the crustal structure and geology. The technique is particularly valuable where sedimentary overburden might conceal important substructure. The New Madrid, Missouri, seismic zone and San Andreas, California, fault zones have been delineated by MT methods.

Special continuous MT monitoring is occasionally employed in active regions where crustal conductivity properties can change. Such measurements have proved useful in active volcanic and seismic fault zones and have the potential of providing warning precursors of major surface disruption. MT techniques have also been used to determine, from the Earth's surface, the burn-front location of fire-damaged coal mines.

CONDUCTIVITY OF THE EARTH'S UPPER MANTLE

For application to conductivity modeling, the size of geomagnetic current sources must be large with respect to skin depth in the probed region. The source must also be well behaved; meaning it must change only slowly and smoothly, in linearly prescribed ways. The quiet-daily variation, *Sq*, currents obtained from field records of standard magnetic observatories meet this requirement as a source for determining the Earth's upper mantle conductivity.

The method of analysis uses the separated external and internal spherical harmonic analysis (SHA) field representation coefficients. The special mathematical properties established for the SHA allow each harmonic to be analyzed independently for the induction response. The method (Campbell, 1987) involves computation of the ratio of the internal to the external components expressed in terms of phase and amplitude and the establishment of a transfer function for producing the conductivity profile from the spherical harmonic coefficients. Then for each SHA coefficient the depth (d, in kilometers) to a layer of conductivity (σ, in siemens per meter) that could be responsible for the induced field measurements is obtained.

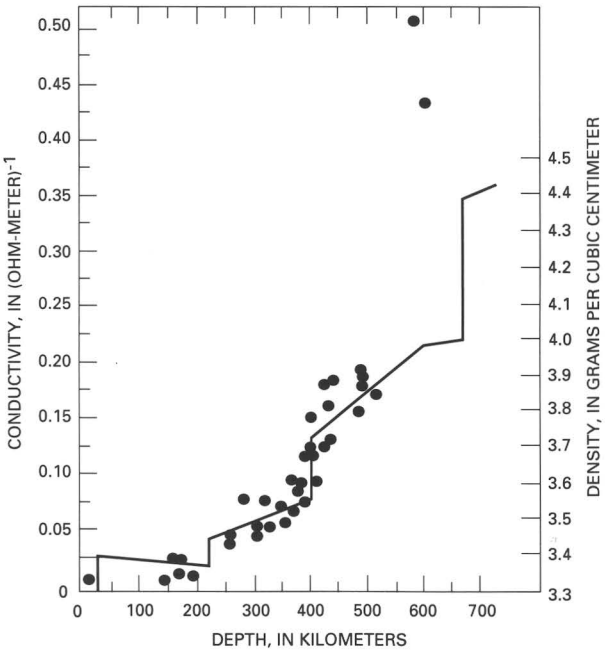

Figure 15. Upper mantle conductivity profile (dots) obtained from analysis of quiet-day geomagnetic records at North American observatories. Solid line segments indicate corresponding values of density obtained from seismic data. Modified from Campbell and Anderssen (1983).

Because the profiles that are obtained are simply the best fit of conductivities (σ) that can produce the same fields, the values are called "substitute" conductors at "equivalent" depths. The reality of the computed values depends on independent corroborating seismic and laboratory evidence. In figure 15, the upper mantle density, obtained from seismic data for the same depth range, is plotted together with the substitute electrical conductivity. The similarity in pattern changes with depth supports the assumption of a true representation of the upper mantle conductivity profile determined from the magnetic fields.

Measurement of electrical conductivity by geomagnetic procedures, established independent of seismic evidence, provides valuable insight into upper mantle composition. Conductivity values can differentiate between materials determined as possible compositions for the Earth's structure by high-temperature and -pressure laboratory modeling.

PALEOMAGNETIC AND ARCHAEOMAGNETIC STUDIES

Ocean-bottom mapping of mid-ocean ridges, which represent the spreading zones of continental drift, shows recurring field-direction patterns that extend perpendicular

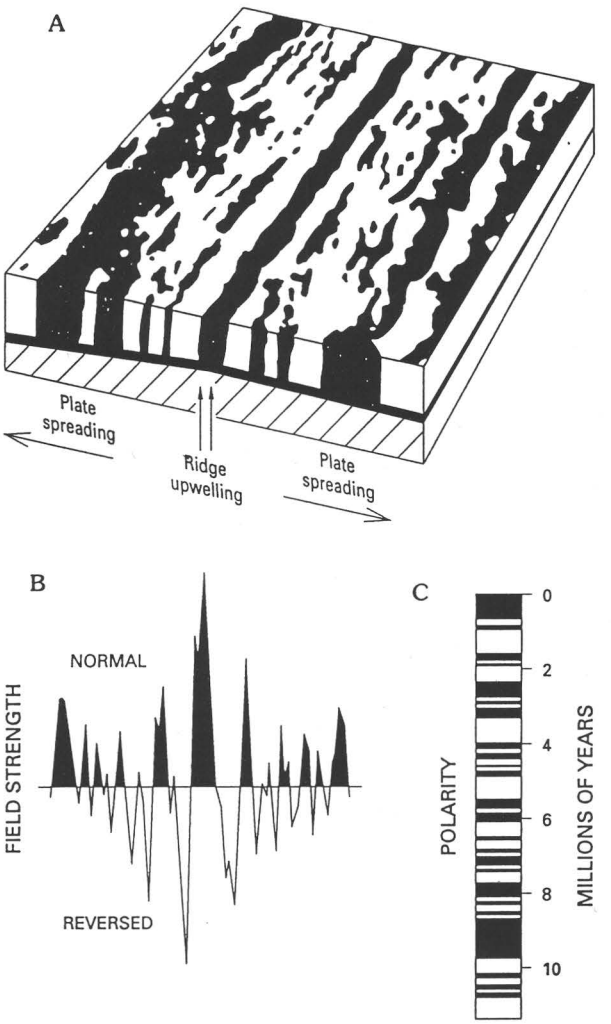

Figure 16. Reversal patterns for the Reykjanes Ridge south of Iceland Modified from Heritzler and others (1966) (modified from Tarling, 1971). *A*, Schematic of pattern. *B*, Field strength from single traverse. C, Polarity time sequence assuming spreading rate of 1 cm/year.

to the spreading axis. Molten mantle materials at temperatures above the Curie point (the temperature at which magnetization is lost) extrude into the ridge and harden, locking in a record of the main field at the time of cooling. Gradually, at about 1–3 cm/year, this upwelling zone lays down a "magnetic tape recording" of ancient magnetic field directions that clearly shows reversal patterns back many millions of years (fig. 16). For regions where the present spreading rate is established, a consistency assumption provides a preliminary dating of reversals. The present field direction is called "normal," the opposite direction "reversed."

Paleomagnetic reversals of field over time form an irregular pattern, much like tree growth rings, that can be matched to samples of unknown date to establish their time

of formation or matched between similarly dated samples to fix their tectonic movement. In some cases, established polar wandering curves must be used to determine the likely age of a group of rocks taken from a single, tectonically stable block. Global patterns of continental drift, established from the paleomagnetic evidence, give record of the formation our planet. Relationships have been established, dating back 800 million years, between paleomagnetic field intensity changes (obtained from deep-sea sediment cores), the Earth's orbital eccentricity, and climatic changes (Wollin and others, 1977).

Archaeological materials that acquired a magnetic remanence at an earlier time when they were heated (such as bricks or clay pots) can be matched with the historical geomagnetic field intensity and direction to fix the sample age. Dating as far back as 5,000 years is possible. For the last century, about 1° in changed field direction represents 5 years of age. Sample remanence can also be used to reconstruct pot-shard and archaeological structure positions by establishing parallel magnetic vector orientations.

MAGNETIC CHARTS

Charting of the changing Earth's surface magnetic field has been a necessary and regular function of the major nations of the world since the early days of global exploration. Typically, contour lines of equal (isomagnetic) increments of field are plotted. Because mercator projections preserve azimuthal relationships, magnetic field declination is best represented on such maps. For consistency, other field components are similarly displayed. Figures 17*A* and *B* are examples of some USGS field charts for 1990 made for popular illustration purposes (more detailed technical charts are the most commonly used products).

Regular changes of the field that occur over a period of years are called "secular changes." These changes can result from change in the current magnitude or area of the principal current loop within the Earth, shift in the alignment of the dipole axis (the dipole North Pole is moving about 18 km northward and 5 km westward each year), and westward drifting of the non-dipole part of the main field. The present westward drift of the geomagnetic pole location (nearly 0.04° per year) is consistent with paleomagnetic evidence that the Earth's dipole and spin axes may coincide about every 10^4 years. The motion of the dipole about the spin axis is called "precessional drift." All these changes require constant recharting of the Earth's field at 5-year intervals with information of the expected linear corrections to be made between charting epochs.

If the dipole field components are removed from a model, the remaining field (non-dipole field) shows contours that drift westward at a rate of about 0.1° each year, much faster than the dipole field. This drift would cause anomalies to circle the globe in about 3,000 years were it not for the fact that the non-dipole anomaly forms may be noticeable altered in less than 100 years. On average, the non-dipole components are changing by about 50 gammas per year. There is some evidence that the anomalies may be severely modified in form as they pass the Pacific Ocean region. Accurate registration of the Earth's field has only been possible for the last 100 years, so our understanding of the drift of these regional features is quite limited. The drifts are used by paleomagneticians to determine the processes within the liquid outer core that generate the Earth's main field.

A correlation coefficient of 0.9 has been established between the change in westward drift and the change in Earth rotation speed several years earlier (1.0 represents perfect correlation, and 0 represents no correlation). The correlation has been ascribed to differences in the rotation speed of the Earth's mantle, outer core, and inner core. There is some evidence that the time variations of the larger Gauss coefficients, representing the spherical harmonic analysis of the modeled main field, showed a relatively sharp change in slope in 1970 (compared to other years), which has been called the "geomagnetic jerk." The explanation, in terms of Earth core and mantle processes, has been exciting considerable research interest.

The global IGRF and DGRF (International and Definitive Geomagnetic Reference Fields) models are usually tabulated to spherical harmonic analysis internal polynomial degree and order 12 (although analyses are carried to higher levels) because, at about that level, the higher polynomials begin to reflect Earth crustal anomalies. Those anomalies of small size, less than about 100 km, generally have been correlated with geological surface features. The field effects of these anomalies disappear rapidly with altitude and make very little, if any, contribution to the space environment. The reference field models are subtracted from area surveys to provide the geologist with crustal conductivity charts.

Buried in the geomagnetic observatory records are annual and semiannual changes. These systematic changes can be caused by the seasonal deformation of the magnetosphere by the particles and fields arriving from the Sun and by the equinoctial-month preference of solar-terrestrial disturbance activity interactions. The separation of internal and external parts in the spherical harmonic analysis of the field helps remove most of these distortions from the internal representation; however, a part of the disturbances induces currents within the conducting Earth that are not so simply removed. Adjustments to the spherical harmonic coefficients are made using empirical relationships to a global activity index, *Dst*, determined from records of selected standard, land-based observatories. The induction contributions to the main-field analysis would be responsible for an 11-year solar-cycle fluctuation in the field model coefficients.

The major problem for the main-field analysis, the poor distribution of surface observations, was originally thought to be solved by a new reliance on satellite measurements of

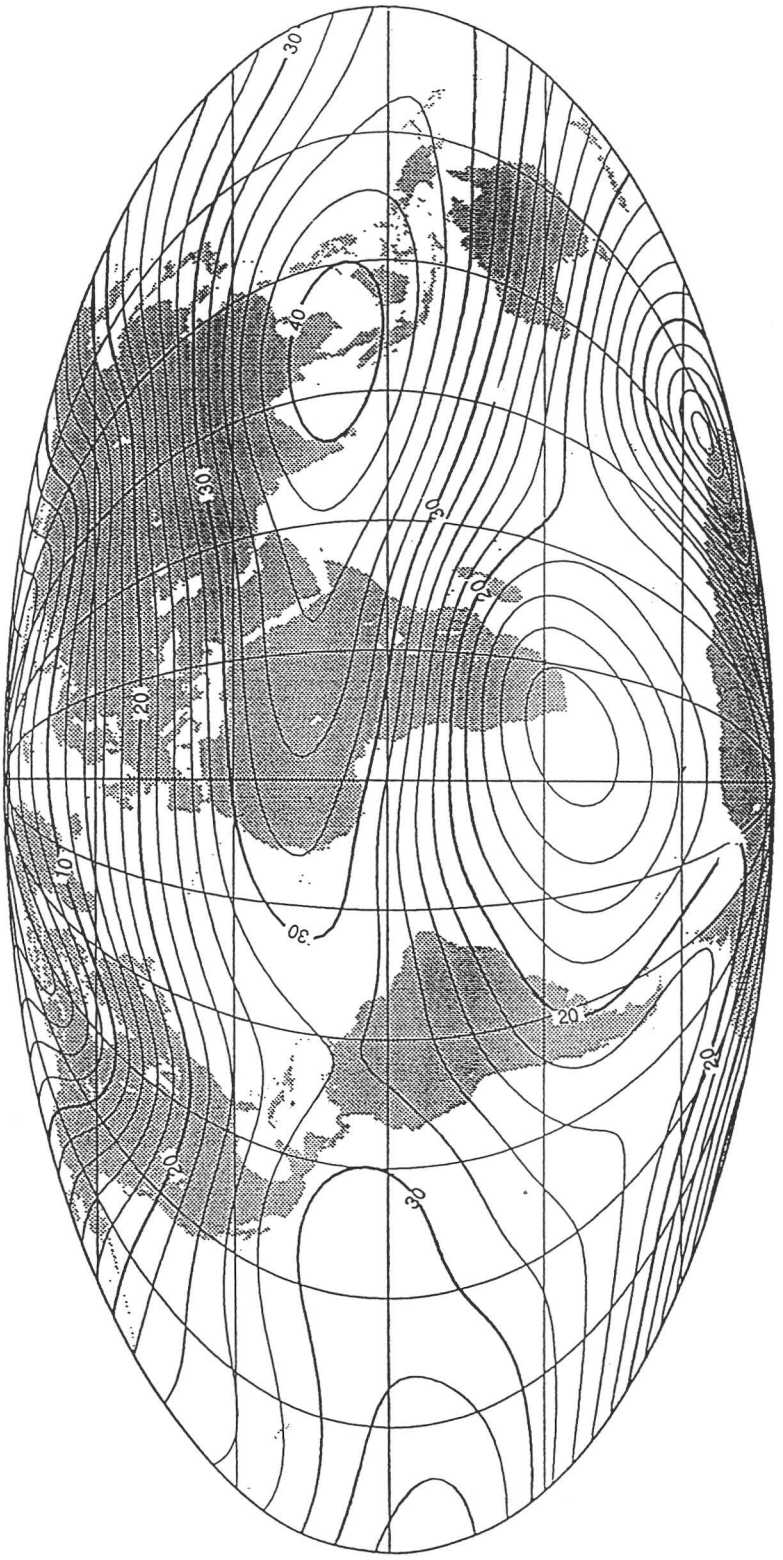
30
40
30
30
20
10
30
20
20
20
30

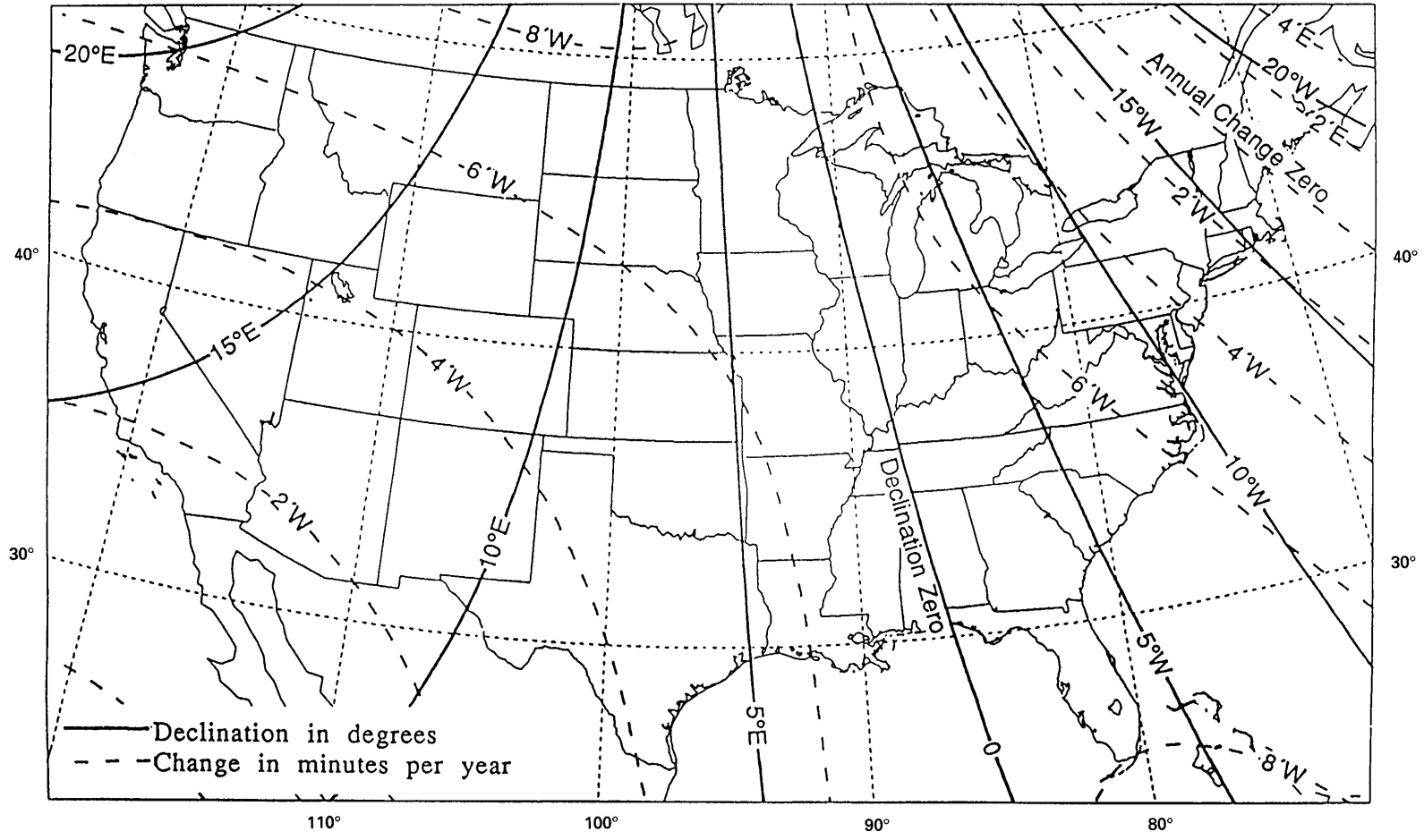

Figure 17. Horizontal intensity of geomagnetic field contoured for global presentation (facing page) and continental United States (above, this page). Courtesy of N. Peddie (USGS, 1994).

the Earth's field from space; however, such measurements have introduced their own unique problems. Internal to the satellite orbit are ionospheric dynamo and auroral electrojet currents as well as high-latitude electrojet and field-aligned currents; the satellite data determined internal (main) field is therefore contaminated by sources that are avoided at surface observatories. Satellite lifetimes are short with respect to surface observatory locations, thus curtailing most secular-change determinations.

Special corrections to the satellite data must be made because one of the requirements for the application of the spherical harmonic analysis is that no currents passed across the surface of analysis. For satellite altitudes of 500 km or more, at higher latitudes strong currents flow along the Earth's field lines through the analysis region. Presently the ground and space data are best combined for the magnetic field analysis epochs.

Most countries provide maps of their respective areas at various levels of detail. Global and U.S. magnetic fields are determined by the USGS every 5 years. These charts are available to the public, at nominal cost, from the USGS in Denver.

NAVIGATION BY MAGNETIC CHARTS

Originally, the compass was a necessary part of maritime navigation. A ship's latitude could usually be determined at night from the elevation of stars in the region of North or South Pole zenith; however, fixing the ship's longitude depended on a daytime determination of the difference between the time of highest Sun elevation and the ship clock time, set when leaving home port. Between the night and daytime latitude-longitude determinations, and in overcast conditions, the ship navigated with the compass. The prime years of global oceanic exploration fostered designs of improved ship clocks for better longitude fixes. The east-west distortions of charts from those times give evidence of those early errors in longitude.

Using maritime charts of the global field, the magnetic declination angle (difference between geographic north and the compass direction) became both a method for guiding the ship's course and for verifying a longitude determination. Global magnetic charting became a major government-supported science. Ships equipped with advanced technology now use the GPS satellite positioning, yet most of the world's ocean-going vessels still navigate with the magnetic compass and charts. All major countries of the world provide magnetic charts as navigational aids for their maritime fleets. Although our flight maps also contain magnetic declination information, the information is rarely used by large aircraft except as a traditional means for identifying airport runway names; small aircraft, however, use compass readings and magnetic chart information for inflight course alignment.

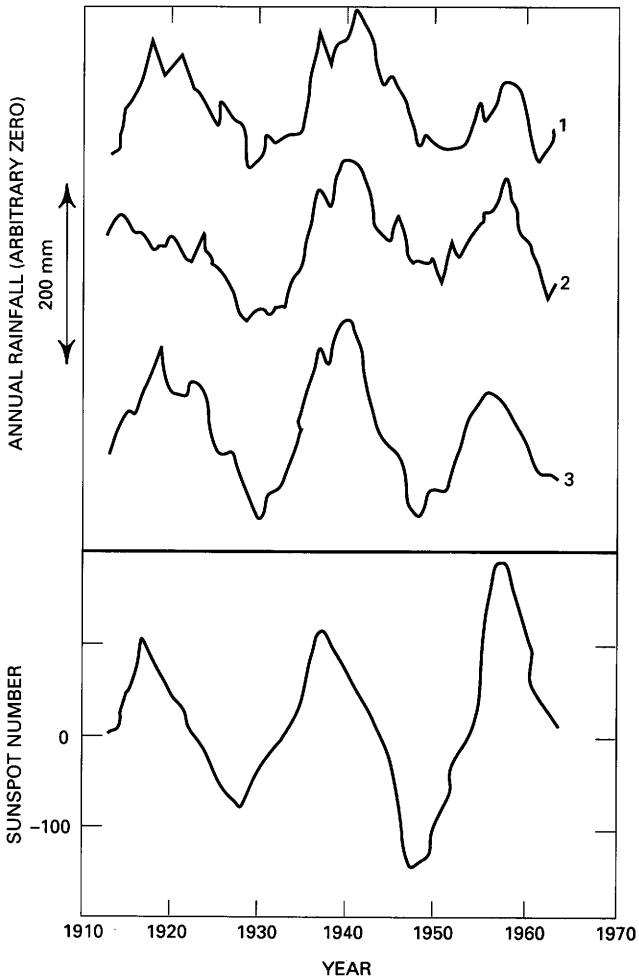

Figure 18. Smoothed annual total rainfall at three locations in South Africa compared with double sunspot cycle. Locations: (1) Rustenburg (lat 26° S., long 27° E.); (2) Bethal (lat 27° S., long 30° E.); and (3) Dundee (lat 28° S., long 30° E.). Modified from King (1975) (reported in Herman and Goldberg, 1978).

The North and South Pole positions and the non-dipole field anomalies move steadily westward at differing rates. These changes require constant recharting of the declination (along with contours of the anticipated annual rate of change) every 5 years. Knowledge of the local magnetic declination is in constant use throughout the world. Almost all topographic maps of small areas contain, along with the date of map production, a graphic indication of the magnetic declination (and annual change) for the area. Seasoned backcountry travelers use a map and compass to establish their routes. Surveyors still make note of compass alignments; some older property lines, originally run with only compass headings, have had to be recreated from historic magnetic information. The use of magnetic field charts continues to be a necessary part of modern man's activities.

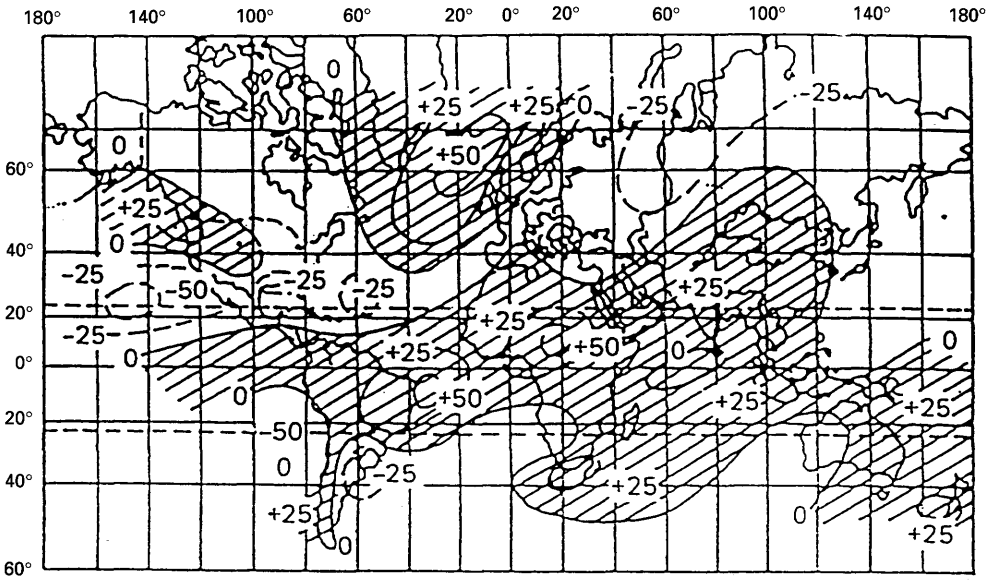

Figure 19. Global annual rainfall difference (in centimeters) between sunspot maximum and sunspot minimum, 1860–1917. Diagonal-lined area is greater rainfall at maximum. Modified from Claton (1923) (reported in Herman and Goldberg, 1978).

GEOMAGNETISM AND WEATHER

Year-to-year changes in growing season length, tree-ring separation, temperature, rainfall, thunderstorms, storm tracks, and winds show clear year-to-year fluctuations relative to sunspot (or double-sunspot) cycles (figs. 18–20). Northern Hemisphere annual mean temperatures are lowest near sunspot maximum and highest near sunspot minimum. Tropopause height over the western Pacific region varies, in phase, with the sunspot cycle. At equatorial latitudes, average annual rainfall is greater during years of solar maximum. Droughts in the western United States follow a 22-year sunspot cycle. Courtillot and others (1982) showed a relationship between the secular variation of the geomagnetic field and the global temperature from 1860 to 1980.

There is a well-known co-variation of sunspot (solar) activity and geomagnetic disturbances. From our present knowledge we would expect that the thermospheric heating by electric currents associated with geomagnetic storms would cause global modification of atmospheric pressure, the persistent patterns of which control seasonal weather conditions. Presently, an active research topic is the full understanding of the exact geomagnetic mechanisms by which weather is modified.

Some specific connections between the geomagnetic storm and weather have been established. Figure 21 shows the recurrent high-latitude, Northern Hemisphere pressure changes, 3 days after a geomagnetic storm in winter months. Solar sector boundary crossings (registered as interplanetary magnetic B_y field changes at the magnetospheric boundary)

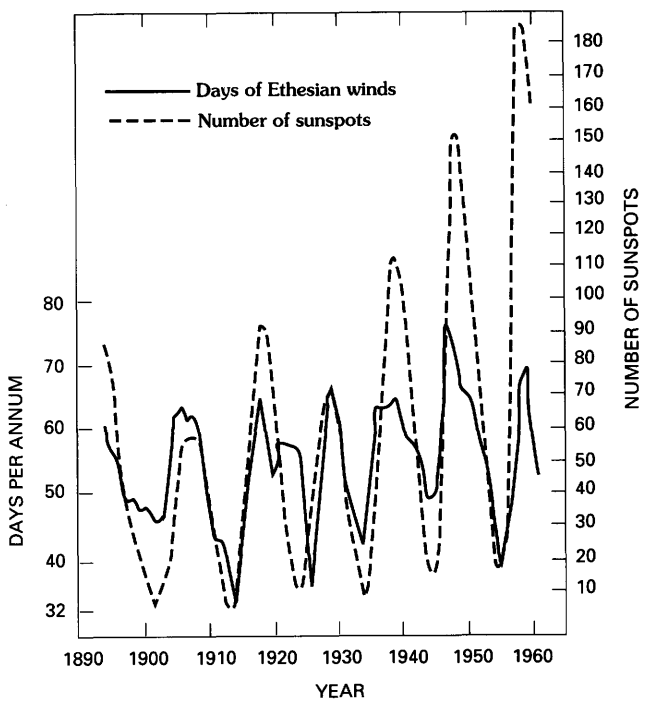

Figure 20. Ethesian winds occurrence, Athens, Greece, 1891–1961. Modified from Carapiperis (1962) (reported in Herman and Goldberg, 1978).

are associated with large increases in geomagnetic activity. Figure 22 shows the systematic decrease in Northern Hemisphere high-latitude atmospheric pressure surfaces about 4 days following a sector boundary crossing. A low-pressure

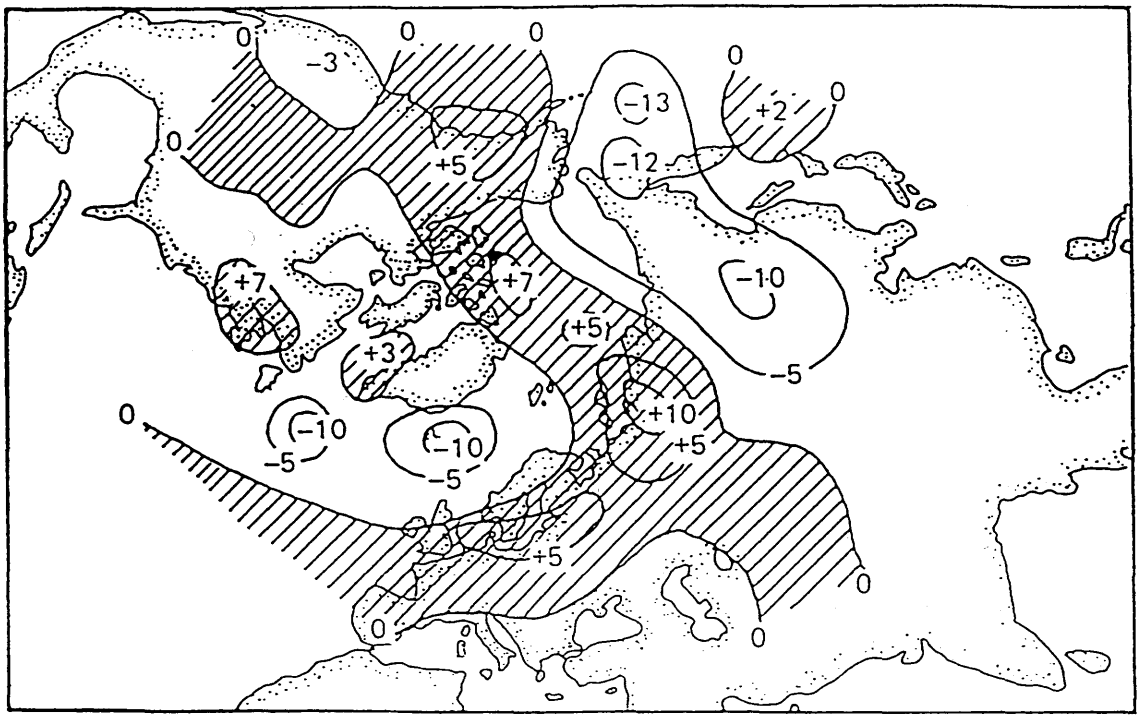

Figure 21. Polar view of averaged surface pressure changes 3 days following 14 geomagnetic storm sudden commencements in the Northern Hemisphere for winter months of 1950–1970. Contours are differences in millibars, and regions of pressure increase are diagonal-lined. Modified from Sidorenkov (1974) (reported in Herman and Goldberg, 1978)

vortex index was determined from the high-latitude Northern Hemisphere area enclosed within the 300-millibar atmosphere pressure contour. Figure 23 shows that the vortex index regularly goes to a minimum value about 1 day after the sector boundary crossing. Global magnetic observatories are a necessary part of the scientific exploration of the weather-field relationship.

GEOMAGNETISM AND LIFE FORMS

In 1974 R.P. Blakemore of the University of New Hampshire discovered freshwater pond magnetotactic bacteria that aimed their movements by sensing the magnetic North Pole direction (Frankel and Blakemore, 1980). During their growth, these bacteria biologically synthesized as many as 20 highly purified cuboidal magnetite crystals, each approximately 50 nanometers in size, arrayed in a dipolar string aligned along the long axis of their bodies. Other magnetotactic bacteria, as well as magnetotactic green alga, were subsequently discovered. The importance of the alga was that, although bacteria do not have a cell nucleus and other cell features, algae and higher organisms do.

The search for similar biological examples of crystalline magnetite subsequently led to discoveries of magnetite in the abdomens of honey bees and in the brains of homing pigeons, tuna, blue marlins, green turtles, dolphins, whales, and others. Honey bees dance to describe locations of their feeding sources; the dances are sensitive to the local magnetic field direction, as well as to the Sun's direction (Gold and others, 1978). There are also indications that the navigation of birds involves a sensing of geomagnetic field direction; homing-pigeon rally organizers, wary of disturbance fields, depend on forecasts of no geomagnetic disturbances to schedule their programs. In 1980, T.P. Quinn of the University of Washington showed that a 90° directional shift in horizontal component of the Earth's magnetic field caused approximately 90° changes in the mean direction of movement of sockeye salmon fry at night. Baker and others (1983) of the University of Manchester discovered magnetite in the ethmoid cavities of humans.

Maugh (1982) reviewed the findings of magnetite in organisms and reported that in mammals, "the investigators found that the magnetic particles appeared to be surrounded by nervous tissue, suggesting the possibility of interaction between the particle and the brain." Kirschvink and others (1985) recently edited a collection of articles on magnetoreception in organisms.

For many years the special superconducting properties of metals had to be studied in liquid helium at temperatures near absolute zero degrees Kelvin (–273°C). Recently, experimenters have developed materials that become

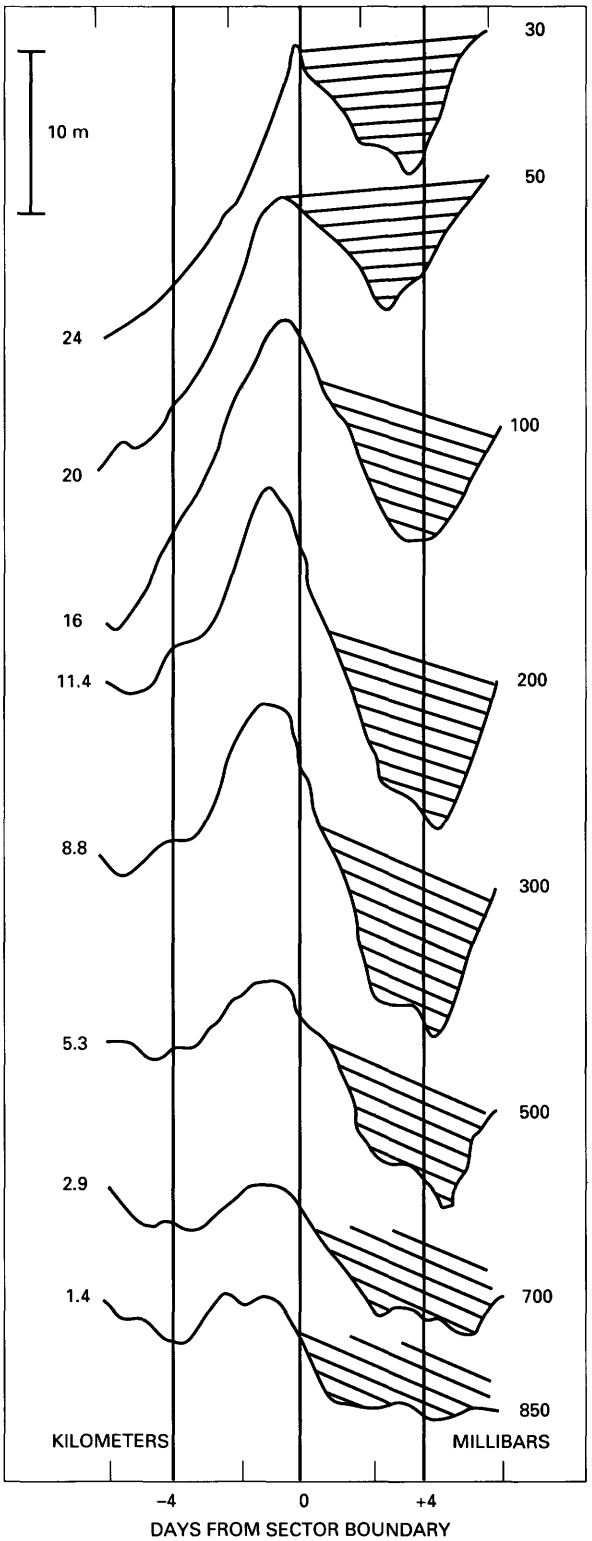

Figure 22. Variation of height difference of pressure surfaces between lat 40°–50° N. and lat 60°–70° N.., before and after a solar magnetic sector boundary passage on day 0, based on superposed epoch analysis of 54 crossings during winters of 1964–1970. Approximate heights (in kilometers) of pressure surfaces (in millibars) are indicated. Modified from Svalgaard (1973) (reported in Herman and Goldberg, 1978).

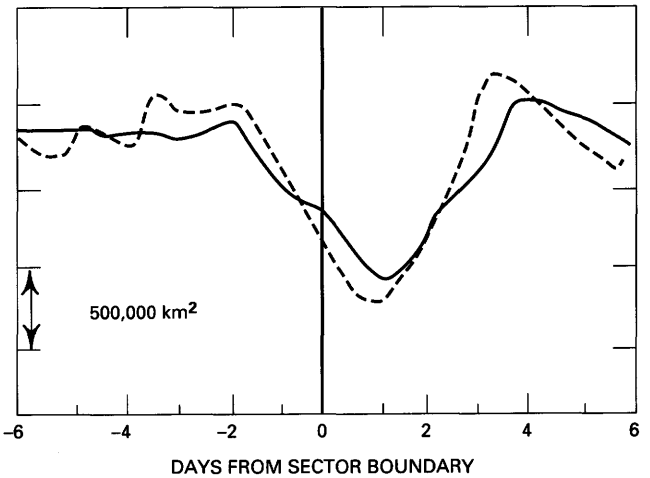

Figure 23. Average response of vorticity area index for magnetic sector boundary passage on day 0. Dashed curve represents 28 boundaries, 1967–1970. Solid curve represents 26 boundaries, 1964–1966. Modified from Wilcox and others (1973) (reported in Herman and Goldberg, 1978).

superconducting at the significantly higher temperature of liquid nitrogen. High-temperature superconducting quantum interference device (SQUID) magnetometers are now being used in medical research to map the magnetic fields associated with human high-order mental functions. Specific response areas of the brain have been identified for cognitive functions, epileptic seizures, Alzheimer's anomalies, and so forth. Brain-wave frequencies span the range of geomagnetic micropulsations and geomagnetic storm oscillations; the geomagnetic fields are considerably more intense than brain waves (fig. 24). The question of whether or not human brain processes respond to external field stimulation has not yet been definitively answered.

There are reports of geomagnetic disturbance effects on man. In a 4-year study, Becker and others (1961) observed a positive correlation between the monthly sums of geomagnetic *K* indices at Fredricksburg and the monthly admissions to two mental hospitals in Syracuse, New York. They found that the probability of obtaining such a relationship by chance was 1 in 1,000. Nikolaev and others (1976) described an extremely interesting study of the psychopathic behavior of inmates at a Moscow mental hospital. From April 1975 through January 1976 each hospital worker contacting patients rated the degree (0 to 5) to which an inmate evidenced his or her psychosis. All numbers were averaged daily for each patient, and a hospital daily average "disturbed condition" index, *S*, was obtained. The daily values of S were compared to the daily geomagnetic *Ap* index, to the polar region geomagnetic field strength, and to polar sector structure indices. Figure 25 shows the increase in disturbed mental behavior of the patients during disturbed geomagnetic field conditions.

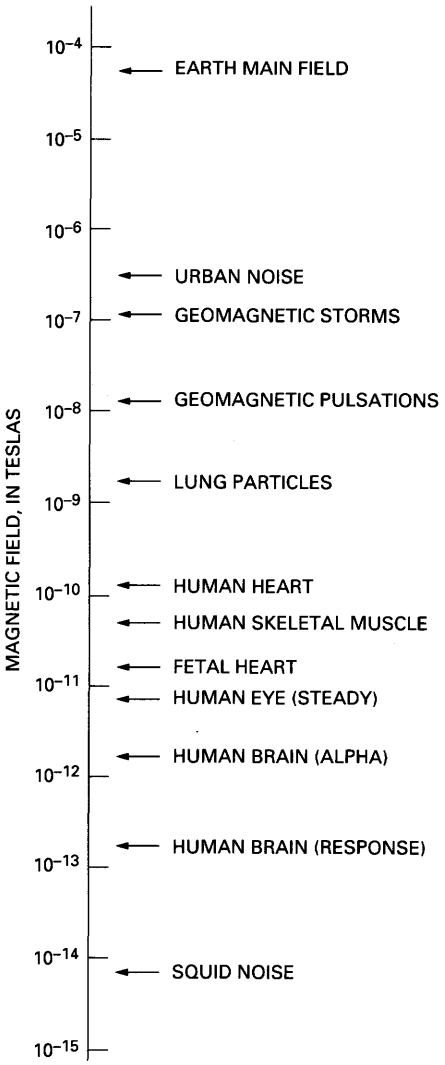

Figure 24. Magnetic fields of the human body compared to geomagnetic field levels and to sensitivity of SQUID magnetometer. Figure redrawn from Williamson and others (1977).

Novikova and Ryvkin (1977) of the Sverdlovsk Medical Institute reported on a 1961–1966 study of the deaths due to myocardial infarction in Sverdlovsk, Russia. Table 1 shows the results of about 3,000 cases of infarction and about 1,000 deaths. On magnetically active days in all years both morbidity and mortality were higher than on magnetically quiet days, with a probability of 0.005 that such a situation was random. For the same study group, Gnevyshev and others (1977) found that the largest number of sudden deaths from cardiovascular disease occurred within the first 24 hours of a geomagnetic storm.

As we look at some of the special effects that have been connected to geomagnetic storms we should keep in mind two cautions. (1) Although associations and correlations between phenomena are important for the first steps in revealing the basic understanding of the physics of any relationship, correlation does not mean dependence. Many of the related phenomena may exist on separate branches of the development tree or may simply have a similar secondary variation; for example, two phenomena, each exhibiting only a seasonal change for different reasons, could show a statistical correlation. (2) Random associations of the averaged behavior of geophysical and biological phenomena can occur. Correlations should not be taken as definitive relationships but rather as interesting possible subjects for further independent investigation.

Table 1. Percentage of days with cases of disease or death from myocardial infarction in Sverdlovsk, Russia, as a function of active and quiet geomagnetic conditions.
[Data from Novikova and Ryvkin (1977)]

	Morbidity		Mortality	
Year	Active	Quiet	Active	Quiet
1961	78.8	70.4	24.5	18.8
1962	73.5	65.3	35.0	25.7
1963	77.6	73.2	24.9	20.6
1964	62.0	57.0	36.4	21.7
1965	79.1	75.0	27.9	25.3
1966	90.8	75.4	59.5	40.9

MAGNETIC OBSERVATORIES

Magnetic observatories throughout the world (fig. 26) operate primarily on national funding to provide services considered to be of public importance. The present-day objective for magnetic observatories is the digital determination of the vector magnetic field to about 0.1–0.01 gammas resolution and about 2 gammas absolute value at a sampling rate of about one value every minute (and for special rapid variation studies one value every 0.1 seconds). This means that stations transmitting to a storage and retrieval center can first compress data considerably, at least to 10^{-3}–10^{-5} of their original time scale. For stations whose main use is other than warning and forecasting, the recording system can be automated for digital recovery at almost any convenient time, as seldom as once a year. At selected sites valuable for space-weather analysis, immediate data transmission via telephone lines or satellites is used. Although geostationary satellites can schedule interrogations of the remote station throughout the day, polar orbiting satellites permit data to be retrieved on about two passes per day at low latitudes and about once every 2 hours at polar latitudes.

The USGS operates 13 magnetic observatories: 7 in the contiguous United States, 3 in Alaska, and 1 each in Hawaii, Puerto Rico, and Guam (fig. 27). Data from these stations are returned instantaneously to the Golden, Colorado, central collection point by satellite and ground-based electronic

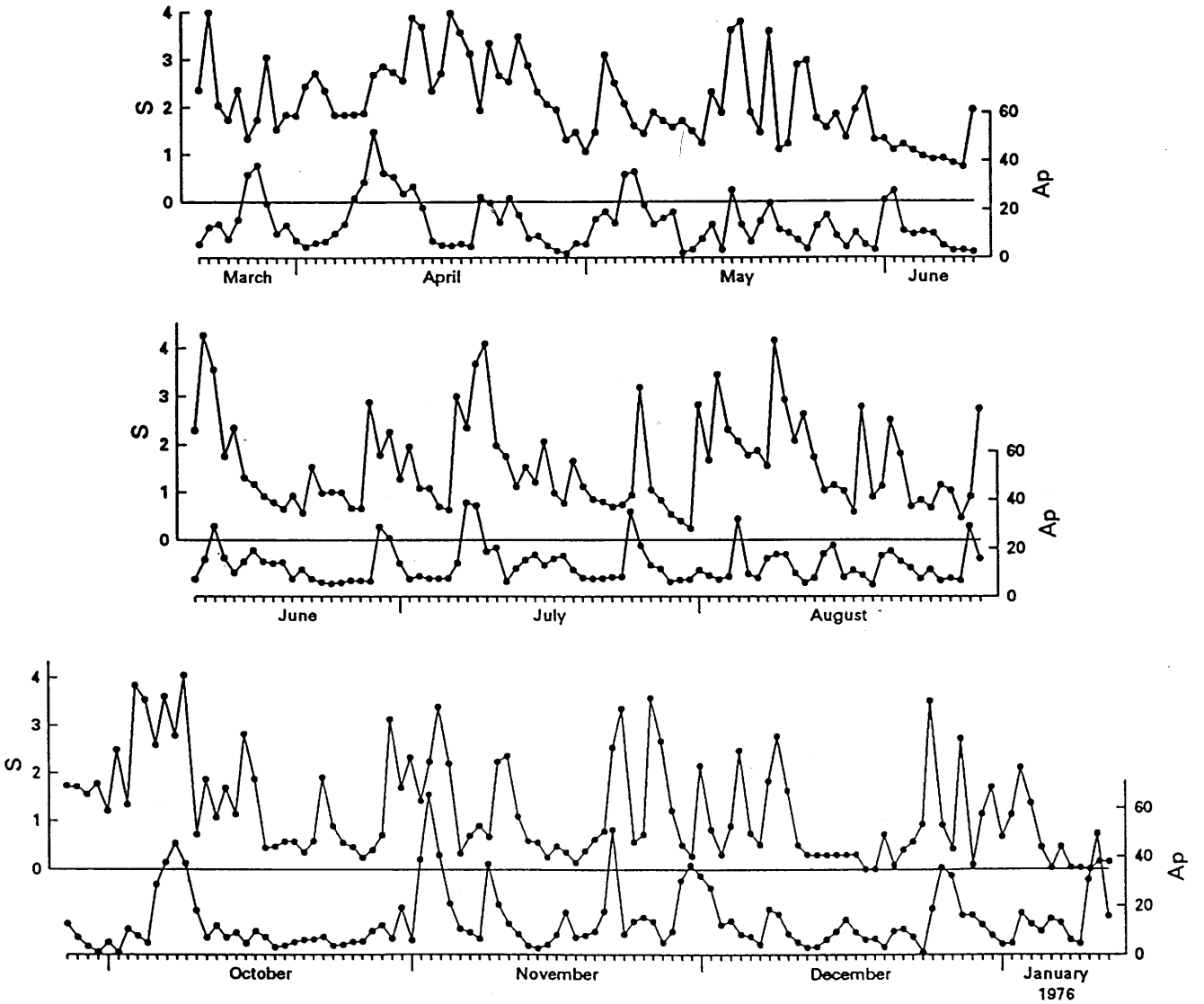

Figure 25. Comparison of group psychopathological syndrome expression index, *S*, at Moscow mental hospital and geomagnetic index, *Ap*, for 9 months of 1975 and 1976. Modified from Nikolaev and others (1976).

communication systems. Data from five of these stations are used in the preparation of the planetary geomagnetic activity indices for worldwide applications. On-line recordings of six of the USGS observatories are provided to the NOAA Space Environment Forecasting Center for integration into its warning and prediction services.

For field modeling and charting, additional geomagnetic measurement sites ("repeat stations") are occupied on a 3–5-year repeated schedule (fig. 27). Special efforts are made at these locations to obtain the best quiet-condition absolute field levels.

World Data Centers (WDC's), started during the International Geophysical Year (1958), are now the prime depositories for most national geophysical records in the form of charts, microfilm copies of charts, tables of values read from the charts, or computer files of digital recordings. The principal centers for archiving of the geomagnetic records are in Boulder, Colorado (WDC-A), Moscow, Russia (WDC-B), and Kyoto, Japan (WDC-C). Geomagnetic records are distributed, free of charge, to organizations that deposit data at the WDC's and, for a small fee, to other individuals or organizations. Besides archiving and distributing geomagnetic records, these centers perform a great number of other services of importance to national and research requirements, such as producing indices, converting geomagnetic data to application formats for easy digestion, and collating related solar-terrestrial phenomena. Geomagnetic data from U.S. observatories are carefully edited, cleaned of extraneous noises and quality checked at the USGS before deposition at WDC-A. In return for this

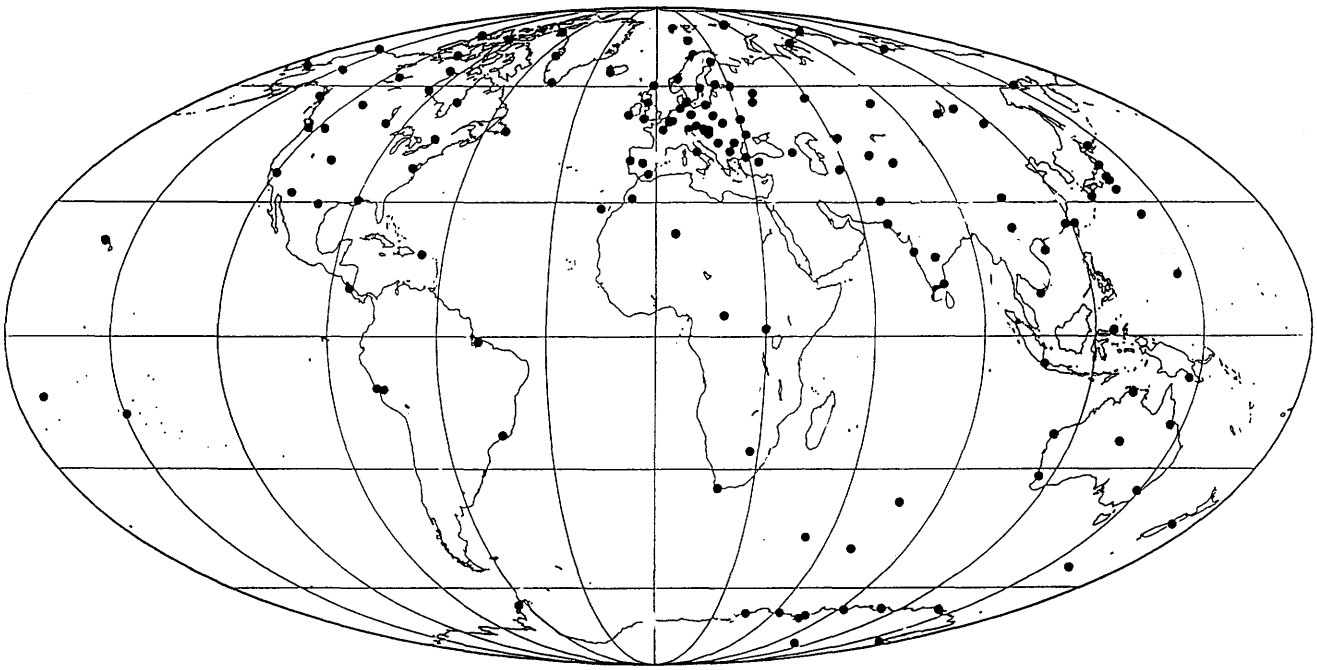

Figure 26. Global magnetic observatory locations depositing records in World Data Center–A in 1994. Courtesy of S. McLean and M. Davis (World Data Center–A, 1994).

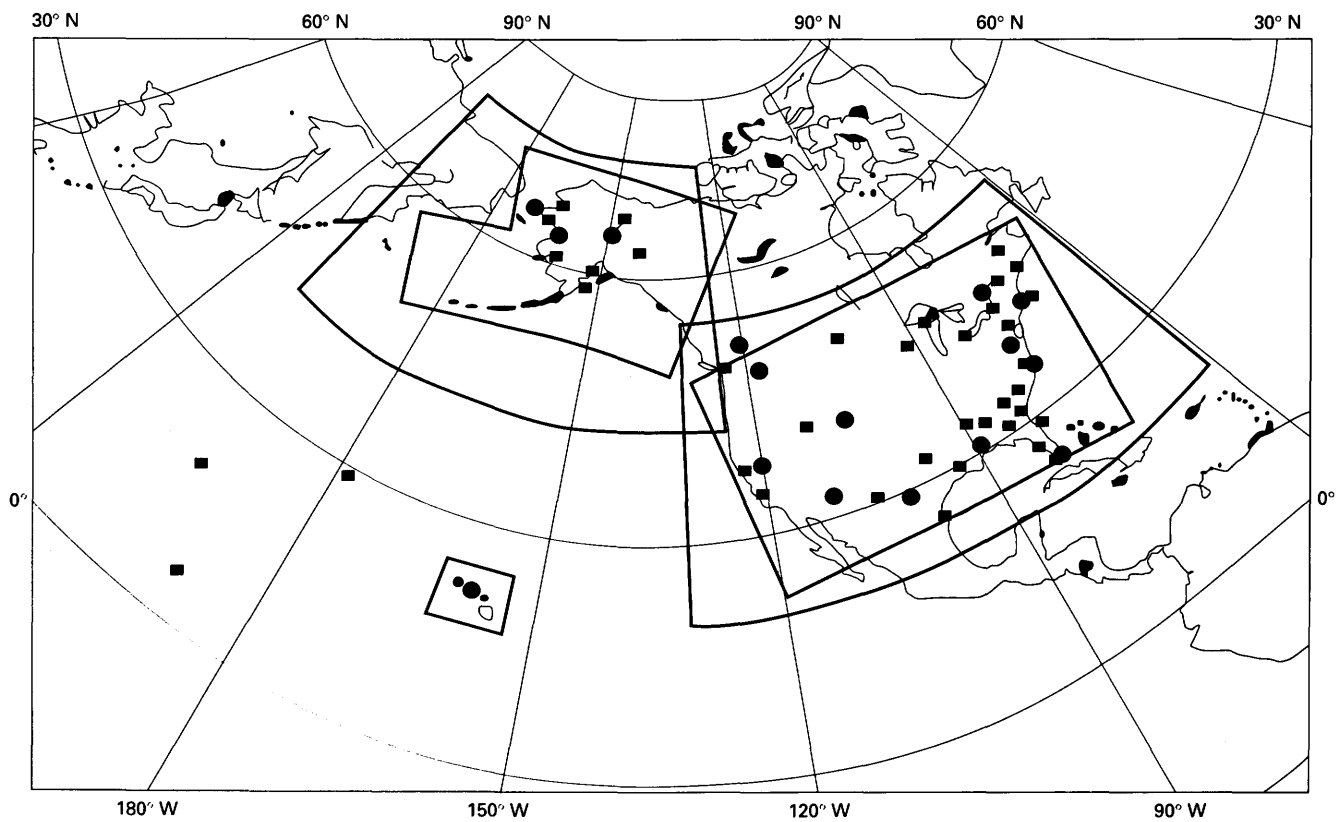

Figure 27. Locations of USGS standard magnetic observatories (solid circles) and sites occupied repeatedly for mapping purposes (solid squares).

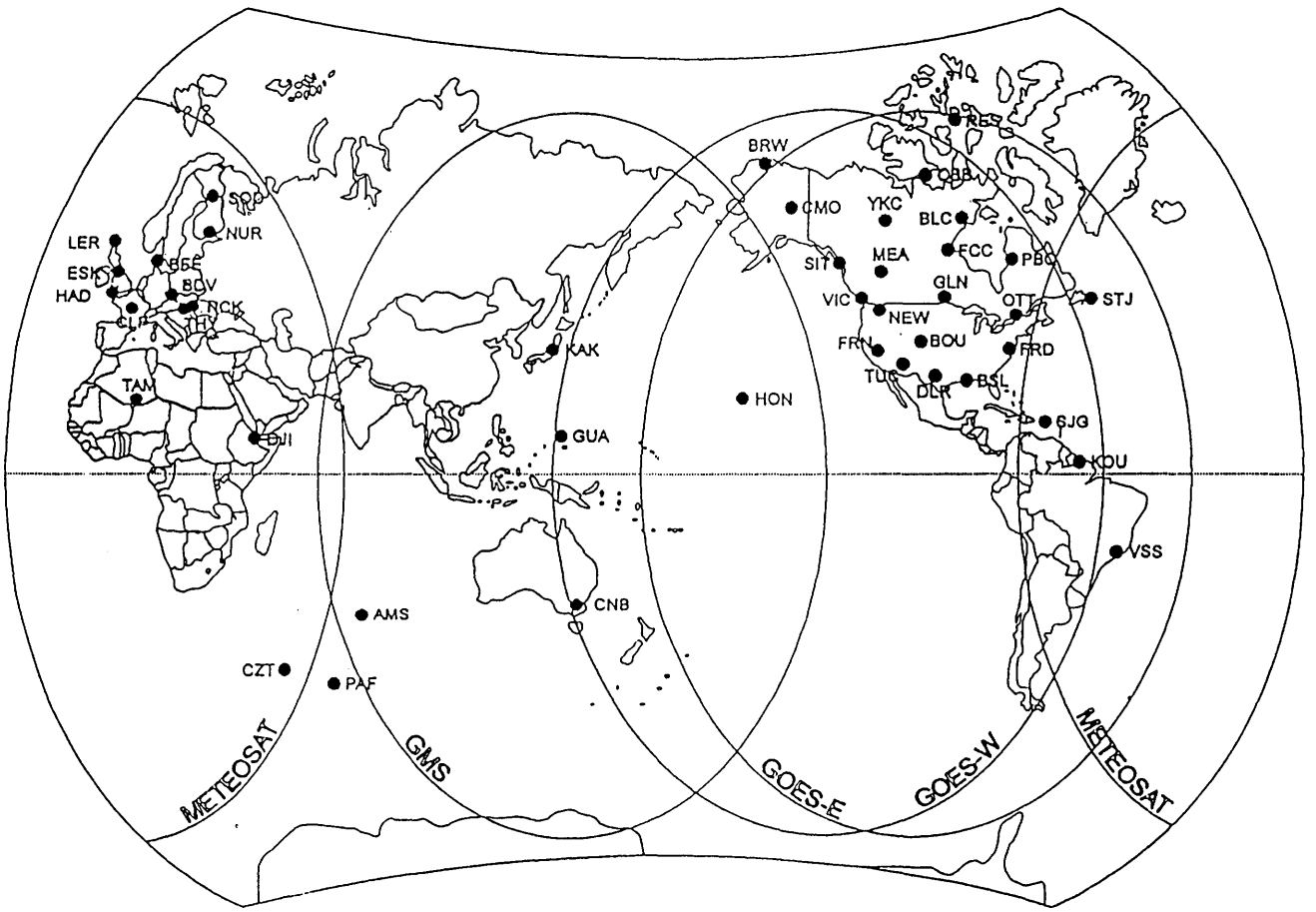

Figure 28. Locations of INTERMAGNET observatories operating in 1993 and reception range (footprints) of four geostationary satellites servicing these observatories. Courtesy of A. Green (USGS).

submission, the USGS obtains copies of other world geomagnetic records from WDC-A archives for global mapping and research purposes.

In recent years a consortium of national geomagnetic observatory leaders, led by the USGS, have arranged a cooperative satellite data recovery system, from about 40 observatories, called INTERMAGNET (international real-time magnetic observatory network). Figure 28 shows the 1994 distribution of the contributing stations and participating satellites. One-minute digital data from INTERMAGNET observatories are broadcast, at 12-minute and 1-hour intervals, to special geostationary satellites within the observatory transmission signal reception window. At selected locations called GIN's (geomagnetic information nodes), these data are collected from the satellite transmissions and distributed to participating agencies. Immediate preliminary appraisal of selected INTERMAGNET recordings provides an important part of the NOAA Space Environment Forecasting Center evaluation of the present and expected space weather affecting satellites, communication, and electric power transmission. After detailed data cleaning and quality checking, computer readable files of archived INTERMAGNET data are collated and made available to the public.

TROPOSPHERIC AND IONOSPHERIC FIELD OBSERVATIONS

About 60 successful rockets have been launched through the high-conductivity layers of the atmosphere for the purpose of measuring ionospheric currents. Most of these flights were designed to study the equatorial electrojet; the others were about equally divided between studies of the auroral electrojet, *Sq* currents, and the main field. Difficulties in obtaining platform stability, accurate orientation determinations, and exact trajectory tracking information have restricted instrumentation to total-field measurements. On occasion, a fluxgate or optically pumped magnetometer is used; however, the proton magnetometer has been a favorite for rocket measurements of ionospheric fields because of its relative simplicity, low weight and cost, insensitivity to temperature and voltage fluctuations, and relative

Table 2. Some features of principal satellites used for geomagnetic field mapping.
[Data from R. Langel and J. Heirtzler (Goddard Space Flight Center, National Aeronautics and Space Administration)]

Satellite	Instrumentation (nanotestlas)	Type	Inclination	Altitude (kilometers)	Operation
COSMOS–49	Proton (22)	Scaler	50°	261–488	October–November 1964.
OGO–2	Rubidium (6)	Scaler	87°	413–1,510	October 1965–September 1967.
OGO–4	Rubidium (6)	Scaler	86°	412–908	July 1967–January 1969.
OGO–6	Rubidium (6)	Scaler	82°	397–1,098	June 1969–July 1971.
MAGSAT	Fluxgate (22)	Vector	97°	325–550	November 1979–May 1980.
DE–2	Fluxgate (100)	Vector	90°	309–1,012	August 1981–February 1983.
UARS	Fluxgate (20)	Vector	57°	574–579	September 1991–Present.
POGS	Fluxgate (30)	Scaler	90°	~700	January 1991–October 1993.
FREJA	Fluxgate (30)	Vector	63°	595–1,759	October 1992–Present.

independence of sensor orientation. Thus far, rocketborne field observations have been limited to magnetometer sensitivity levels of a few gammas.

Penetration of the ionospheric current carrying layers is indicated by the difference between the measured field and that expected from an inverse-cube-law decrease of the Earth's field (determined from the global field models) with increasing height. Successful flights reach well above the 100–120 km current layer to about 250 km. The E-region location of ionospheric dynamo currents and the auroral and equatorial electrojet currents has been verified by rocketborne magnetometers. The influence of these currents on surface observatories has been interpreted from the rocket measurements. This information has led to better use of surface observatories as ionospheric disturbance monitors.

MAGNETOSPHERIC MEASUREMENTS

Equatorial and polar satellites are generally restricted to far above 300 km for atmospheric drag reasons; 600–2,000-km altitudes and 1.5–3.5-hour orbits are typical. Geostationary satellites are limited to about 6.6 R_e distance in the equatorial plane. The geostationary GOES weather satellites have become monitoring platforms for sampling local high-energy particles, X-rays, and geomagnetic fields. On occasions of a major solar-terrestrial disturbance, the day-side magnetospheric boundary may be pressed in past this geostationary position, providing shock-boundary crossing measurements for the in situ magnetometer and important disturbance and forecasting information. Interpretation of the surface observatory records has been confirmed by comparisons with satellite field measurements. As a result, standard surface observatories have become the continuous, and less expensive, magnetospheric process monitors.

Polar-orbiting satellite magnetometers make significant contributions to global magnetic field mapping. The problems in space are the detection of a small ambient field in the presence of spacecraft noise and the separation of spatial from temporal field changes. The inclination of these satellites (the angle between the Earth's spin axis and the perpendicular to the plane of the orbit) should be close to 90° to provide full coverage of the Earth. An inclination value greater than 90° is used to indicate a rotational path of the satellite opposite to the Earth's rotation direction. An error in the pointing direction of the field sensors of 5 arc seconds can introduce a 1.5-nT error in measurements. Trajectory errors are mostly due to limitations in tracking-station timekeeping and to changes in satellite acceleration with varying magnetospheric conditions. At a typical satellite velocity of about 7 km/second, a 0.1-second time accuracy translates to 700-m location accuracy along the track and 4.2-nT difference in total field.

Early satellite geomagnetic field measurements were of the total-field (scaler) type made with "absolute" field measuring proton or rubidium magnetometers. In recent years, satellites have used the three-axis (vector) fluxgate magnetometers calibrated with collocated absolute sensors to about 2–5 gammas. The sensors are usually placed on a boom 2–8 m from the body of the spacecraft whose attitude in space is determined with a star sensor and (or) GPS. A mechanism is then needed to monitor the magnetometer location with respect to the body of the spacecraft. The main electronics needs to operate in the range of about –10°C to +50°C. Table 2 lists some of the features of the principal satellites that have, to date, provided significant global field mapping information.

Several additional magnetic field missions are planned at this time. The POGS measurement are to be continued from 1996 to 2000 with improved sensor designs on Defense Meteorological Satellite Program (DMSP) spacecraft. In September 1995 the Danish OERSTED satellite is to be launched for an approximately 14-month-long mission. OERSTED will use scalar proton and vector fluxgate magnetometers in an elliptical 400–800-km polar orbit that is to drift slowly from a nearly Sun synchronous position. The SAC-C satellite with a vector fluxgate magnetometer is planned for a 1998 launch into a polar orbit at about 500–600 km altitude. A group of three small satellites (STEDI) projected for lauch in 1997–97 will have

Table 3. Daily forecast of geomagnetic storm conditions and subsequently observed conditions, 1989–1991.
[Values courtesy of K.A. Doggett (National Oceanic and Atmospheric Administration, Space Environmental Laboratory). Storm conditions are defined as daily $Ap>50$]

	Observed	
Forecast	No-storm	Storm
No-storm	1,052	23
Storm	12	7

magnetometers aboard. A tethered staellite series, SEDS, is also expected to have magnetometers.

Satellite observations that encompass the full Earth have the great advantage of a global coverage unmatched by surface observatories; however, several drawbacks limit the prospect for total reliance on satellite measurements for charting of the Earth's magnetic field. Field values are dependent on position accuracy of the fast-moving space platform, and satellite fluxgate instruments are 100 times less sensitive than the modern surface observatory system. Because of the satellite position above the current-carrying ionosphere, the external and internal parts of Earth's field, computed from spherical harmonic analysis, place the ionospheric currents interior to the satellite and thereby degrade a main-field determination. The best world-field models are obtained from a combination of the satellite and surface station records.

SOLAR-TERRESTRIAL DISTURBANCE PREDICTIONS

As the applications of geomagnetism to human activity increase, there is a corresponding growth in the global appetite for reliable predictions. Sufficient archived geomagnetic information is stored at the World Data Centers to allow accurate long-term statistical predictions (such as the number of daily disturbances of more than 100 gammas during a 40-year period in a specific region of the world). Solar-cycle predictions of the year and level of next year's average geomagnetic activity also can be provided with reasonable certainty. Forecasters do well in their appraisal of the average activity level for the next rotation of the Sun (about 27 days) and for the possible arrival of activity seen on the solar limb. All these predictions are important for protective designs of manmade systems sensitive to geomagnetic disturbances.

Problems arise with prediction of onset time, activity level, and disturbance duration of specific events. The log-normal form of the *Dst* index allows some estimate of storm recovery levels from recordings of the initial rise to maximum disturbance level. From the tracking of solar activity and coronal mass ejections, some storm prediction success has been accorded to the space-environment forecasters in their predictions of disturbed conditions for the next hour, day, and week. Table 3 lists the results of daily forecasts of storm conditions (daily *Ap* index greater than 50) for the period 1989 through 1991.

The 98.9 percent accuracy of the no-storm prediction is related to the high occurrence of quiet days and to the fact that easily observed quiet-Sun conditions always guarantee a low in geomagnetic variations. Predictions of suitable days for observatory baseline measurements, aeromagnetic flights, pipeline cathodic protection measurements, and so forth are highly reliable. Of the 30 storm days, 77 percent were not predicted. As long as temporary movement to a protective operational mode is not costly, many storm-sensitive systems are already benefiting from even the poor storm-prediction accuracy.

Although disturbance forecasting is a developing science, equally important to users is detailed "nowcasting," an accurate apparisal of the present space conditions. Relying on these data, space programs, communication systems, power-distribution facilities, and so forth take protective actions that save millions of dollars of public and private funds. A vital part of the nowcasting capability is the input from the USGS and INTERMAGNET geomagnetic observatory programs.

The disturbance forecasting capability will be greatly improved by the placement of special satellites downstream in the solar wind. There is a position, called the Lagrange point L_1, about 1.5×10^6 km from the Earth (at 235 R_e it is about 1/100 of the distance to the Sun), where a satellite can circle the Sun in 1 year and appear to be relatively fixed in the Sun-Earth line. The first satellite, called WIND for solar wind, was launched in November 1994 for daily sampling of particles of fields. The second satellite at this location, called ACE for advanced composition explorer, is to be launched in 1997 and will provide continuous real-time data transmission of full solar wind particle and field information. Knowledge of incoming wind composition, velocities, and field directions are necessary for determining the reaction of the magnetosphere to solar-terrestrial disturbances.

The physics of the disturbed field and particle conditions from the Sun to the Earth's surface is still not fully revealed. Each year and new solar cycle brings us closer to a full understanding of solar-terrestrial processes and to a greater application of geomagnetism to societal needs. The system of national solar-terrestrial disturbance forecasting centers has made a major contribution to this endeavor. Forecasting improvement techniques presently rely on enlarging the collection of selected surface observatory and space data in near real time. For the future, we can expect that our knowledge of the details of surface geomagnetic field responses will increase with advancement of our understanding of magnetospheric substorms, continuing the vital role of USGS standard magnetic observatories in disturbance forecasting.

SUMMARY AND CONCLUSIONS

Applications of geomagnetism expand as our society grows in its technological capabilities. As our country increases its uses of the space environment, so increases the need for more exact information on the physics of the magnetosphere. This physics is intimately tied to understanding of magnetic field changes as well as monitoring those changes that impact satellite operation. Large geomagnetic storms affect pipelines, power-transmission networks, communication systems, location fixes, and so forth. Magnetic mapping plays a major role in the discovery of mineral resources and specification of their emplacement. Solid-earth geophysics relies on geomagnetism for revelation of our Earth's formation and change. Geomagnetism is beginning to play a role in atmospheric weather and climate modeling. Magnetic charts are continuing their usage in marine navigation. A developing science of magnetoreception in organisms may offer explanation of reported biological responses to geomagnetic fields. The national requirements for geomagnetic disturbance warning and forecasting make growing demands for timely and accurate geomagnetic information on a global scale. Our national U.S. Geological Survey geomagnetic observatory network, the National Oceanic and Atmospheric Administration Space Environment Forecasting Center, and the geomagnetic data archival and retrieval facilities of World Data Center–A work together as a multiuse technology of immense value to our Nation.

REFERENCES CITED

Allen, J.H., Frank, L., Sauer, H., and Reiff, P., 1989, Effects of the March 1989 solar activity: EOS, v. 70, no. 46, p. 1479, 1486–1488.

Allen, J.H., and Wilkinson, D.C., 1992, Solar-terrestrial activity affecting systems in space and on earth: National Oceanic and Atmospheric Administration National Geophysical Data Center internal report, 33 p.

Baker, R.R., Mather, J.G., and Kennaugh, J.H., 1983, Magnetic bones in human sinuses: Science, v. 301, p. 78–80.

Becker, R.O., Bachman, C.H., and Friedman, H.H., 1961, Relation between natural magnetic field intensity and increase of psychiatric disturbances in the human population: International Conference on High Magnetic Fields, Massachusetts Institute of Technology, Cambridge, November 3, 1961.

Blais G., and Metsa, P., 1993, Operating the Hydro-Quebec grid under magnetic storm conditions since the storm of 13 March 1989: Solar-Terrestrial Predictions Workshop, 4th, Ottawa, Canada, May 18–22, 1992, Proceedings; National Oceanic and Atmospheric Administration, U.S. Department of Commerce, v. 1, p. 108–130.

Campbell, W.H., 1986, An interpretation of induced electric currents in long pipelines caused by natural geomagnetic sources of the upper atmosphere: Surveys of Geophysics, v. 8, p. 239–259.

———1987, The upper mantle conductivity analysis method using observatory records of the geomagnetic field: Pure Applied Geophysics, v. 125, p. 427–457.

Campbell, W.H., and Anderssen, R.S., 1983, Conductivity of the sub-continental upper mantle—An analysis using quiet day geomagnetic records of North America: Journal of Geomagnetism and Geoelectrics, v. 35, p. 367–382.

Campbell, W.H., Schiffmacher, E.R., and Kroehl, H.W., 1989, Global quiet day field variation mode WDCA/SQ1: EOS, Transactions of the American Geophysical Union, v. 70, no. 5, p. 66–74.

Courtillot, V., LeMouel, J.L., Ducruix, J., and Cazenave, A., 1982, Geomagnetic secular variation as a precursor of climatic change: Nature, v. 297, no. 5865, p. 386–387.

Frankel, R.B., and Blakemore, R.P., 1980, Navigational compass in magnetic bacteria: Journal of Magnetism and Magnetic Materials, v. 15, p. 1562–1564.

Gnevyshev, M.N., Novikova, K.F., Ol', A.I., and Tokareva, N.V., 1977, Sudden death from cardiovascular diseases and solar activity, *in* Effects of solar activity on the Earth's atmosphere and biosphere: Academy of Sciences, U.S.S.R.; English trans., Israel Program for Scientific Translation, Jerusalem, p. 201–210.

Gold, J.L., Kirschvink, J.L., and Deffeyes, K.S., 1978, Bees have magnetic remanence: Science, v. 201, p. 1026–1028.

Gough, D.I., and Ingram, M.R., 1983, Interpretation methods for magnetometer arrays: Reviews in Geophysics, v. 21, p. 805–827.

Heirtzler, J.R., LePichon, X., and Brown J.G., 1966, Magnetic anomalies over the Reykjanes Ridge: Deep Sea Research, v. 13, p. 427–443.

Herman, J.R., and Goldberg, R.A., 1978, Sun, weather, and climate: National Aeronautics and Space Administration Publication SP 426, Washington, D.C., 360 p.

Hruska, J., Coles, R., Lam, H.L., and van Beek, G.J., 1990, The major magnetic storm of 13–14 March, 1989—Its character in Canada and some effects: Report of the Geophysics Division, Geological Survey of Canada, Ottawa.

Kappenman, J.L., 1992, Geomagnetic disturbances and power system effect: Solar-Terrestrial Predictions Workshop, 4th, Ottawa, May 18–22, Proceedings; National Oceanic and Atmospheric Administration, U.S. Department of Commerce, v. 1, p.131–141.

Kirschvink, J.L., Jones, D.S., and MacFadden, B.J., eds., 1985, Magnetite biomineralization and magnetoreception in organisms—A new biomagnetism: New York, Plenum Press, 682 p.

Kleusberg, A., 1993, The global positioning system and ionospheric conditions: Solar-Terrestrial Predictions Workshop, 4th, Ottawa, May 18–22, Proceedings; National Oceanic and Atmospheric Administration, U.S. Department of Commerce, v. 1, p. 142–146,.

Kurtz, R.D., Delaurier, J.M., and Gupta, J.C., 1990, Electrical conductivity distribution beneath Vancouver Island—A region of active plate subduction: Journal of Geophysical Research, v. 95, p. 10920–10946.

Lanzerotti, L.J., and Medford, L.V., 1989, Geomagnetic disturbance and long-haul telecommunications cables: Electrical

Power Research Institute Conference on Geomagnetically Induced Currents, November 1989.

Maugh, T.H., II, 1982, Magnetic navigation—An attractive possibility: Science, v. 215, p. 1492–1493.

Nikolaev, Yu.S., Rudakov, Ya.Ya., Mansurov, S.M., and Mansurova, L.G., 1976, Interplanetary magnetic field sector structure and disturbances of the central nervous system activity: Preprint N 17a, Academy of Sciences, U.S.S.R., IZMIRAN, Moscow, 29 p.

Norton, R.B., 1969, The middle latitude F region during some severe ionospheric storms: Proceedings of the Institute of Electric and Electronic Engineers, v. 57, p. 1147.

Novikova, K.F., and Ryvkin, B.A., 1977, Solar activity and cardiovascular diseases, *in* Gnevyshev, M.N., and Ol', A.I., eds., Effects of solar activity on the Earth's atmosphere and biosphere: Academy of Sciences, U.S.S.R.; English trans., Israel Program for Scientific Translation, p. 184–200.

Oldenburg, D.W., 1990, Inversion of electromagnetic data—An overview of new techniques: Surveys of Geophysics, v. 11, p. 231–270.

Quinn, T.P., 1980, Evidence for celestial and magnetic compass orientation in lake migrating sockeye salmon fry: Journal of Comparative Physiology, v. 137, p. 243–248.

Rostoker, G., 1993, Magnetospheric substorms—Their phenomenology and predictability: Solar-Terrestrial Predictions Workshop, 4th, Ottawa, May 18–22, Proceedings, v. 3, p. 21–35.

Schmucker, U., 1970, An introduction to induction anomalies: Journal of Geophysical Research, v. 22, p. 9–33.

Shapka, R., 1993, Geomagnetic effects on modern pipeline system: Solar-Terrestrial Predictions Workshop, 4th, Ottawa, May 18–22, Proceedings; National Oceanic and Atmospheric Administration, U.S. Department of Commerce, v. 1, p. 163–170.

Tarling, D.H., 1971, Principals and applications of paleomagnetism: London, Chapman and Hall, 164 p.

Williamson, S.J., Kaufman, L., and Brenner, D., 1977, Magnetic fields of the human brain: U.S. Naval Research Reviews, October, p. 1–18.

Wollin, G., Ryan, W.B.F., Ericson, D.B., and Foster, J.H., 1977, Paleoclimate, paleomagnetism and the eccentricity of the Earth's orbit: Geophysical Research Letters, v. 4, p. 267–274.

Wrenn, G.L., 1994, Conclusive evidence for internal dielectric charging anomalies on geosynchronous communications spacecraft: Paper presented to Users Conference, National Oceanic and Atmospheric Administration Space Environment Laboratory, Boulder, Colorado, May 2–5.

Published in the Central Region, Denver, Colorado
Manuscript approved for publication September 1, 1994
Edited by Judith Stoeser
Graphics by Shelly Fields and the author
Photocomposition and cover design by Shelly Fields

☆U.S. GOVERNMENT PRINTING OFFICE: 1995- 673-046/86093